GOLD
OPEN ACCESS

THE GEOLOGICAL SOCIETY
OF AMERICA®

Geodynamic models of the West Antarctic Rift System: Implications for the mantle thermal state

Dennis L. Harry[1], Jourdan L. Anoka[2], and Sumant Jha[1]
[1]Colorado State University, Department of Geosciences, Fort Collins, Colorado 80523, USA
[2]Excel Geophysical Services, 5655 S Yosemite St Suite 470, Greenwood Village, Colorado 80111, USA

ABSTRACT

Two-dimensional finite element models simulating extension of the West Antarctic Rift System (WARS) exhibit three classes of behavior, which are dependent upon the pre-rift thermal state of the upper mantle. All of the models begin with relatively cool East Antarctica lithosphere juxtaposed against warmer West Antarctica. The models all undergo an initial period of extension that is broadly distributed across the WARS. Class 1 models continue to extend in this way for more than 80 m.y. before abruptly developing a lithospheric neck at the edge of the model furthest from East Antarctica. The behavior of Class 1 models is dominated by a horizontal temperature gradient caused by juxtaposition of the warm WARS lithosphere against the cooler East Antarctica lithosphere. This produces a corresponding strength gradient, which causes a neck to eventually develop at the warm, weak edge of the model. Class 1 models have relatively high pre-rift temperatures at the base of the crust (>800 °C), which inhibits focusing of strain during the first 80 m.y. of extension. In Class 2 models the rift axis develops within the interior of the WARS. Class 2 models differ from Class 1 models in that the net heat production in the crust plays a larger role in determining the temperature at the top of the mantle prior to and during rifting. Necking at the edge of these models is inhibited because crustal thinning leads to cooling and strengthening of the lithosphere at the edge of the model. This causes the locus of extension to shift toward the weaker interior of the WARS. In Class 3 models, the rift axis forms where the pre-rift lithosphere transitions between relatively cool and thick East Antarctica and warmer and thinner West Antarctica. In these models, syn-extensional cooling and strengthening of the lithosphere causes the locus of strain to shift into the transitional region rather than the interior of the WARS. Class 3 models resemble the evolution of the WARS, which underwent a period of broad extension during the Late Cretaceous through late Paleogene Periods and more focused extension near the West Antarctica/East Antarctica boundary during the Neogene Period. All Class 3 models require the mantle potential temperature during the Late Cretaceous through Paleogene phase of broad extension to be no greater than 1270 °C, suggesting that an active mantle plume was not present beneath the WARS during the early stages of extension.

◼ INTRODUCTION

The West Antarctic Rift System (WARS) is a 750–1000-km-wide continental extensional province lying beneath the Ross Sea and Ross Ice Shelf between Marie Byrd Land on the east and the Transantarctic Mountains (TAM) at the edge of the East Antarctic craton on the west (Fig. 1). The timing and distribution of extension in the WARS are not tightly constrained, particularly beneath the West Antarctic Ice Sheet. However, it is clear that widespread extension began by Late Cretaceous time and continued at least into the Pleistocene Epoch
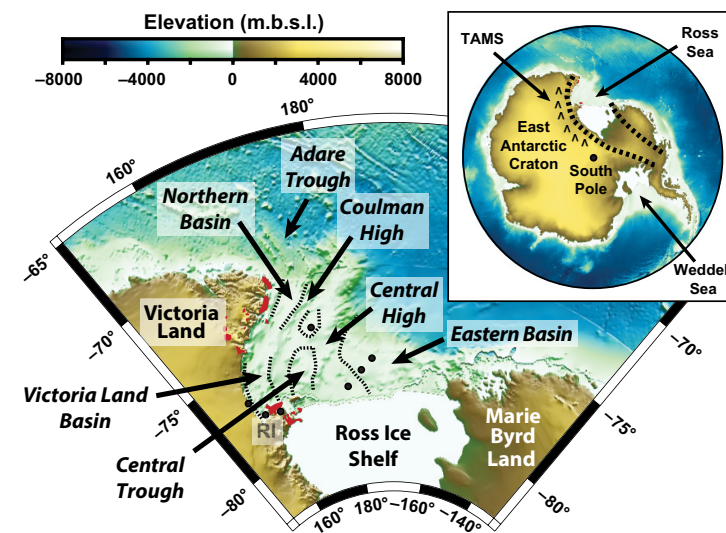

Figure 1. Location map and major tectonic features of the Ross Sea and West Antarctic Rift System (WARS). The Location of the Transantarctic Mountains (TAMS) and boundaries of the WARS (dashed lines) are shown in the inset. Dotted line—Late Cretaceous through Cenozoic basins and uplifts (Davey et al., 2006); black dots—drillholes penetrating Late Cretaceous through Cenozoic stratigraphy; red shading—Cenozoic alkaline magmatic rocks; RI—Ross Island. Relief from ETOPO2 global relief data set (National Geodetic Data Center, 2006).

(Cooper and Davey, 1985; Lawver and Gahagan, 1994; Davey and Brancolini, 1995; Busetti et al., 1999; Cande et al., 2000; Decesari et al., 2008b; Siddoway, 2008). During the Late Cretaceous and Paleogene Periods, extension was distributed irregularly across the breadth of the Ross Sea. Since early Neogene, extension has focused near the sides of the rift, particularly in the western Ross Sea near the boundary between East and West Antarctica (Cooper et al., 1987a; Storey et al., 1992; Davey and Brancolini, 1995; Davey et al., 2000; Hamilton et al., 2001; Fielding et al., 2008b; Hall et al., 2008; Henrys et al., 2008; Nardini et al., 2009; Paulsen et al., 2014).

Cenozoic alkaline rocks emplaced on the flanks of the rift have trace element and isotopic characteristics similar to oceanic island basalts (OIB) (Kyle, 1990; LeMasurier and Rex, 1991; Hole and LeMasurier, 1994; Weaver et al., 1994; Hart et al., 1997; Tonarini et al., 1997). High amplitude magnetic anomalies indicate similar magmatic rocks are widespread beneath the Ross Ice Shelf and Ross Sea, with the total volume of syn-rift magmatic rocks estimated to be comparable to many large igneous provinces (Behrendt et al., 1994, 1996, 1997). The large volume and broad distribution of magmatic rocks emplaced during rifting and the similarities of their trace element abundances to OIB have led some to postulate that a mantle plume or plumes underlay the WARS during all or some of the rifting episode (LeMasurier and Rex, 1991; Behrendt et al., 1994, 1996, 1997; Hole and LeMasurier, 1994; Weaver et al., 1994; Rocholl et al., 1995; LeMasurier and Landis, 1996; Storey et al., 1999; Wörner, 1999; LeMasurier, 2006). This is consistent with relatively low seismic velocities in the upper mantle beneath parts of the WARS (Danesi and Morelli, 2000; Sieminski et al., 2003; Morelli and Danesi, 2004; Lawrence et al., 2006a; Gupta et al., 2009; Accardo et al., 2014; Chaput et al., 2014; Heeszel et al., 2016; O'Donnell et al., 2017). Others, however, have argued that trace element and isotopic trends in the magmatic rocks are more consistent with a metasomatized upper mantle source rather than an upwelling hot mantle plume (Futa and LeMasurier, 1983; Weaver et al., 1994; Rocholl et al., 1995; Hart et al., 1997; Wörner, 1999; Panter et al., 2000; Rocchi et al., 2002, 2005; Finn et al., 2005; Perinelli et al., 2006; Cooper et al., 2007; Nardini et al., 2009; Scott et al., 2014).

Seismic data provide images only of the modern state of the mantle and are unable to distinguish between hot versus compositionally altered mantle. Thus, the question of whether Mesozoic WARS rifting was associated with a mantle plume remains unresolved. An alternative constraint on the syn-rift mantle temperature is offered by geodynamic models, which have shown that the overall structural evolution of continental rifts are sensitive to the pre-rift thermal state of the lithosphere and upper mantle (Braun and Beaumont, 1987, 1989; Bassi, 1991; Buck, 1991; Hopper and Buck, 1993; Buck et al., 1999; van Wijk and Cloetingh, 2002). In this paper, we present a series of finite element models of rifting to investigate the range of lithosphere and upper mantle thermal conditions that are consistent with the mechanical evolution of the WARS. Specifically, we seek to place bounds on the thermal conditions that produce models that simulate an initial prolonged period of broad extension followed by a later period of more focused extension near the East Antarctica/West Antarctica boundary. We show that this mechanical behavior requires asthenosphere potential temperatures no greater than the global average.

■ GEOLOGY OF THE WEST ANTARCTIC RIFT SYSTEM

Geography and Tectonic Setting

From Late Paleozoic time to ca. 105 Ma, the region now occupied by the WARS lay on the overriding plate of a convergent margin between East Gondwana and the Phoenix Plate (Lawver et al., 1992; Lawver and Gahagan, 1994) (Fig. 2). The extensional tectonic setting and modern crust thickness in the Ross Sea (~20–22 km average—Trey et al., 1999; Chaput et al., 2014; Heeszel et al., 2016) suggest that the region had relatively thick crust (>35 km) prior to extension. This has led to the inference that, prior to extension, the WARS and neighboring Zealandia formed an elevated orogenic plateau behind the convergent margin that was similar in scale to the modern Andean Altiplano (Studinger et al., 2004; Bialas et al., 2007; Fitzgerald et al., 2008; Huerta, 2008; Wilson and Luyendyk, 2009; Wilson et al., 2012a). The presence of an elevated plateau is not universally accepted (e.g., Lisker and Laufer, 2013), but the presence of a thicker crust throughout most of the WARS prior to extension appears to be required if crust volume is conserved (or, as is more likely in the WARS, if crust volume slightly increased due to magmatic intrusion).

A brief period of back-arc extension occurred between 180 and 175 Ma, coincident with the early stages of the breakup of Gondwana and emplacement of the Ferrar magmatic rocks in an elongate belt parallel to the western margin of the rift (Elliot, 1992; Studinger et al., 2004; Ferraccioli et al., 2009). Widespread and persistent extension began ca. 105 Ma, when the Phoenix-Pacific spreading ridge collided with the East Gondwana margin (Storey et al., 1992; Davey and
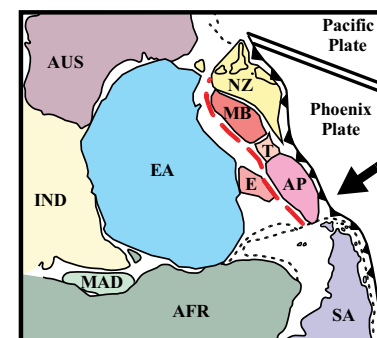

Figure 2. Late Cretaceous reconstruction of west antarctic Gondwana margin ca. 110 Ma showing early collision of Phoenix/Pacific spreading system with New Zealand. Red dashed line shows trend of incipient West Antarctic Rift. SA—South America; AFR—Africa; IND—India; AUS—Australia; EA—East Antarctica; NZ—New Zealand. Major tectonic blocks comprising West Antarctica are: AP—Antarctic Peninsula; E—Ellsworth Mountains; T—Thurston Island block; MAD—Madagascar; MB—Marie Byrd Land. Modified after Fitzgerald (2002) and Torsvik et al. (2008).

Brancolini, 1995; Luyendyk, 1995; Eagles, 2003; Eagles et al., 2004, 2009; Torsvik et al., 2008). Faults, mylonites, redbeds, and alkaline magmatic rocks indicate that broadly distributed extension continued throughout the WARS and Zealandia at least until New Zealand separated from Marie Byrd Land ca. 85 Ma ~~(Lawver and Gahagan, 1994; Weaver et al., 1994; Luyendyk et al., 1996; Cande et al., 2000; Luyendyk et al., 2001; Larter et al., 2002; Luyendyk et al., 2003; Kula et al., 2007; Siddoway, 2008; Siddoway et al., 2004; Schwartz et al., 2016)~~.

It is uncertain whether extension continued into the Paleogene, or if the latest Cretaceous through early Cenozoic was a period of tectonic quiescence ~~(Cooper and Davey, 1985; Cooper et al., 1991; Lawver and Gahagan, 1994; Davey and Brancolini, 1995; Fitzgerald, 2002)~~. In either case, accumulations of thick faulted strata in the Ross Sea and magmatism on both flanks of the rift make it clear that extension was again (or still) under way in the Eocene ~~(Cooper and Davey, 1985; Cooper et al., 1991; Davey and Brancolini, 1995; Busetti et al., 1999; Davey et al., 2000)~~. Seismic reflection profiles in the Ross Sea image four major N-S–striking fault bounded basins (from west to east, the Victoria Land Basin/Northern Basin, Central Trough, and Eastern Basin) that in composite form the broad WARS extensional province (Fig. 1). Drilling shows these basins to be filled with up to 14 km of strata ranging up to Middle Eocene in age, with un-drilled deeper strata on the seismic profiles inferred to be Paleocene or Late Cretaceous ~~(Barrett et al., 1987; Bartek et al., 1996; Wilson et al., 1998, 2012b; Hamilton et al., 2001; Powell et al., 2001; Roberts et al., 2003; Barrett, 2007; Naish et al., 2007; Acton et al., 2008; Decesari et al., 2008a; Fielding et al., 2008a, 2008b)~~. On the western margin of the WARS, Paleogene extension in the Victoria Land and Northern basins was coeval with and structurally linked to seafloor spreading in the Adare Trough to the north of the western Ross Sea between 43 and 26 Ma (Cande et al., 2000; Davey et al., 2006, 2016; Granot et al., 2010, 2013).

A Late Oligocene unconformity separates Paleogene and older syn-rift strata from Neogene strata in the Ross Sea ~~(Barrett et al., 1987; Bartek et al., 1996; Hamilton et al., 2001; Powell et al., 2001; Roberts et al., 2003; Barrett, 2007; Naish et al., 2007; Acton et al., 2008; Decesari et al., 2008a; Fielding et al., 2008a, 2008b; Wilson et al., 1998, 2012b)~~. Strata below the unconformity thicken toward the basin axes, onlap the interbasin highs, and are faulted throughout the Ross Sea, indicating extension across the breadth of the WARS during Paleogene time. The Neogene strata dominantly record broad post-rift thermal subsidence, indicating an end of extension by Late Oligocene time across most of the WARS. Extension continued into the Neogene Period on the margins of the rift. On the western margin, the Terror Rift in the central Victoria Land Basin contains Miocene and younger strata that are much thicker than in the more easterly basins, and normal faults cut through the entire sedimentary sequence ~~(Cooper and Davey, 1985; Cooper et al., 1987b, 1991; Trey et al., 1999; Hamilton et al., 2001; Müller et al., 2005; Fielding et al., 2008b; Hall et al., 2008; Henrys et al., 2008; LeMasurier, 2008)~~. Neogene extension was accompanied by a continuation of the alkalic magmatism in the western WARS/TAM region that began in the Paleogene Period, renewed alkalic magmatism in Marie Byrd Land ~~(Hole and LeMasurier, 1994; Weaver et al., 1994; Tonarini et al., 1997;~~

~~Mukasa and Dalziel, 2000; Rocchi et al., 2002; Nardini et al., 2009; Armienti and Perinelli, 2010)~~, and a change from an extensional to transtensional stress regime ~~(Wilson, 1995; Jones, 1996; Salvini et al., 1997; Müller et al., 2007; Rossetti et al., 2006; Paulsen and Wilson, 2009; Paulsen et al., 2014)~~. The faults and ongoing alkaline magmatism show that extension in the Terror Rift continued at least until the Pleistocene Epoch, and may be ongoing today.

Structure of the Lithosphere and Upper Mantle

The crust thickness has been estimated from gravity data, surface wave tomography, and receiver functions. On the east flank of the rift, in Marie Byrd Land, the crust is 25–30 km thick (Winberry and Anandakrishnan, 2004; Chaput et al., 2014; O'Donnell and Nyblade, 2014; An et al., 2015). The thickness of the crust in the interior of the WARS is variable, ranging from 10 to 21 km in the Ross Sea basins, up to 24 km beneath the inter-basin highs, and as great as 37 km in the un-extended Ellsworth Mountains block between the Ross Sea Embayment and Weddell Sea Embayment ~~(Davey, 1981; McGinnis et al., 1985; Davey and Brancolini, 1995; Trey et al., 1999; von Frese et al., 1999; Bannister et al., 2000, 2003; Ritzwoller et al., 2001; Llubes et al., 2003; Ferraccioli et al., 2011; Jordan et al., 2013, 2017; O'Donnell and Nyblade, 2014)~~. On the west side of the rift, the crust thickness increases westward from 25 to 34 km near the Ross Sea coast (on the western flank of the Victoria Land Basin) to 35–40 km beneath the TAM. The crust within the interior of East Antarctica, outside of the WARS tectonic domain, ranges from 34 km near the South Pole to 40–60 km in the central East Antarctic craton ~~(Behrendt and Cooper, 1991; Busetti et al., 1999; Trey et al., 1999; Bannister et al., 2000; Ferraccioli et al., 2001; Ritzwoller et al., 2001; Bannister et al., 2003; Llubes et al., 2003; Winberry and Anandakrishnan, 2004; Lawrence, 2006b; Studinger et al., 2006; Hansen et al., 2009, 2016, 2010; Pyle et al., 2010; Finotello et al., 2011; Chaput et al., 2014; An et al., 2015; Graw et al., 2016)~~.

Surface-, S-, and P-wave tomography shows the upper mantle beneath the WARS to have lower average seismic velocities than beneath East Antarctica ~~(Danesi and Morelli, 2000; Ritzwoller et al., 2001; Sieminski et al., 2003; Morelli and Danesi, 2004; Winberry and Anandakrishnan, 2004; Lawrence et al., 2006a; Watson et al., 2006; Hansen et al., 2014; An et al., 2015; Heeszel et al., 2016; O'Donnell et al., 2017)~~. No broad regional plume-like features are evident in the seismic velocity structure at wavelengths greater than 200 km, but narrower low-velocity anomalies are present beneath Marie Byrd Land (extending to >400 km depth) and Ross Island (extending to ~200 km depth) ~~(Danesi and Morelli, 2000; Sieminski et al., 2003; Morelli and Danesi, 2004; Watson et al., 2006; Hansen et al., 2014)~~. The Marie Byrd Land velocity anomaly is consistent with a 200–300-km-wide plume sourced within or below the mantle transition zone (Hansen et al., 2014; Lloyd et al., 2015). The Ross Island anomaly is elongated northward and southward parallel to the TAM front, and extends inland 50–100 km from the coast (underlying the TAM) (Danesi and Morelli, 2000; Morelli and Danesi, 2004; Lawrence et al., 2006b; Watson et al., 2006;

Gupta et al., 2009; Hansen et al., 2014). Fast uppermost mantle velocities are observed beneath the rift basins in the Ross Sea, consistent with their inferred pre-Neogene age (high velocities indicate post-rift cooling) (Lloyd et al., 2015). An exception is the Bentley Subglacial Trough in the eastern WARS, where slow upper mantle velocities indicate Neogene extension (Emry et al., 2015; Lloyd et al., 2015). Modern heat flux data are sparse and variable, with most data ranging from 70 to 115 mW m^{-2} within the WARS and adjacent regions near the Transantarctic Mountain Front (~~Blackman et al., 1987; Berg et al., 1989; Behrendt and Cooper, 1991; Vedova et al., 1992; Busetti et al., 1999; Bucker et al., 2001; Morin et al., 2010; Schroder et al., 2011~~).

A decrease in shear-wave velocities at the top of the asthenosphere indicates that the lithosphere is ~80–100 km thick in the central WARS and 200–220 km thick in East Antarctica (Roult et al., 1994; Morelli and Danesi, 2004; Lawrence et al., 2006a). The velocity structure beneath the TAM and the region bordering the East Antarctica coast of the Ross Sea is transitional between that of the stable, cool, and thick East Antarctic lithosphere and the warmer, thinner, and more recently tectonically active West Antarctic lithosphere. The relatively thin crust and low upper mantle seismic velocities that characterize the WARS extending inland ~50–100 km from the coast to beneath the central TAM (Bannister et al., 2003; Winberry and Anandakrishnan, 2004; Lawrence et al., 2006b; Watson et al., 2006).

Magmatic History of the WARS

In Marie Byrd Land, alkaline magmatism associated with extension began soon after the Pacific-Phoenix spreading ridge collided with the Mesozoic convergent margin ca. 100 Ma (Weaver et al., 1994; Davey and Brancolini, 1995; Mukasa and Dalziel, 2000). These early-rift alkaline rocks are enriched in less-compatible trace elements compared to mid-ocean ridge basalts (MORB), with Nd isotopic compositions indicating source enrichment between 500 and 600 Ma, and trend toward more depleted trace element geochemical signatures with decreasing age. Cenozoic alkalic magmatism occurred on both flanks of the rift, beginning ca. 48 Ma in Northern Victoria Land and ca. 30 Ma in Marie Byrd Land, and continuing into the present (~~LeMasurier and Rex, 1991; Hole and LeMasurier, 1994; Mukasa and Dalziel, 2000; Rocchi et al., 2002; Rilling et al., 2008; Nardini et al., 2009~~). The Late Cretaceous and Cenozoic mafic igneous rocks in the WARS region have trace element distributions similar to those of ocean island basalts, being enriched in large ion lithophile elements compared to MORB. The broad distribution of syn-rift igneous rocks and their geochemical attributes have led to the suggestion that a mantle plume, or multiple plumes, are responsible for syn-rift magmatism in the WARS, at least during the Cenozoic Era (~~LeMasurier and Rex, 1991; Esser et al., 2004; Hole and LeMasurier, 1994; Weaver et al., 1994; LeMasurier and Landis, 1996; LeMasurier, 2006, 2008~~). The argument for a modern plume or plumes is supported by aeromagnetic data that indicate up to 5×10^5 km^3 of magmatic rocks of inferred Cretaceous or younger age beneath the Ross Sea

and Ross Ice Shelf (Behrendt et al., 1994; Behrendt et al., 1996; Behrendt et al., 1997), by seismic tomographic images showing narrow low velocity regions in the mantle (Sieminski et al., 2003; Hansen et al., 2014), and by uplift of the Marie Byrd Land Dome since Late Oligocene time (LeMasurier, 2006).

Rocchi et al. (2005) noted that, given the long duration of rifting, the rate of melt production is much less than in most large igneous provinces that have been associated with mantle plumes. Thus, a hot mantle plume is not necessary to explain the large volume of magmatic rocks within the WARS, although a long-lived fertile magma source would be required instead. Furthermore, although a Cenozoic plume is advocated by many, it is not clear that a plume is required to explain Late Cretaceous magmatism. Decompression melting of lithospheric mantle that was metasomatically enriched during the long period of subduction prior to the Late Cretaceous Period has been proposed (~~Weaver et al., 1994; Panter et al., 2000, 2006; Rocchi et al., 2002, 2005; Perinelli et al., 2006; Armienti and Perinelli, 2010; Aviado et al., 2015~~), as has melting of a heterogeneous asthenosphere containing pockets of fertile metasomatized material or fossil remnants of an older (pre-rift) mantle plume (~~Rocholl et al., 1995; Hart et al., 1997; Wörner, 1999; Finn et al., 2005; Cooper et al., 2007; Nardini et al., 2009~~), melting of rising asthenosphere beneath the subducted Phoenix-Pacific spreading system (Mukasa and Dalziel, 2000), and successive melting of a geochemically stratified mantle that includes depleted asthenosphere, enriched lithosphere, and fossil plume sources (Rocholl et al., 1995; Wörner, 1999; Perinelli et al., 2006; Aviado et al., 2015).

■ PREVIOUS GEODYNAMIC MODELS OF RIFTING

Buck (1991) showed that extension of thick continental crust tends to favor formation of broad extensional provinces rather than narrow rift zones. The reasons for this are twofold. First, a thick crust leads to relatively high temperatures at the top of the mantle. High temperatures minimize lateral differences in strength, inhibiting strain localization that is required to initiate necking (formation of a narrow region of focused lithospheric thinning). Second, with necking poorly developed, crustal thinning is distributed over a relatively broad area and the rate of thinning is concomitantly low. As a result, the upper (lithospheric) mantle beneath the thinning crust has time to cool during extension, becoming stronger and promoting a shift in extension to adjacent regions. The continuously and perhaps progressively shifting loci of extension combine to produce a broad extensional province (Harry et al., 1993; Hopper and Buck, 1996; van Wijk and Cloetingh, 2002). In contrast, a relatively thin crust leads to a relatively cool upper mantle. At cool upper mantle temperatures, structurally or compositionally induced lateral variations in strength in the uppermost mantle become relatively pronounced. Small variations in, for example, crust thickness, lead to localization of strain. With extension localized in a narrow area, crustal thinning progresses rapidly. This inhibits cooling and strengthening of the upper mantle, causing deformation to remain localized and promoting formation of a narrow rift.

Extrapolating these model behaviors to the pre-rift WARS provides an understanding of the Late Cretaceous through late Paleogene period of broadly distributed extension throughout the WARS. Toward this end, Bialas et al. (2007) explored a series of finite element models to simulate the Cretaceous phase of broad extensional collapse of a postulated WARS orogenic plateau. Their models, which have a relatively thick pre-rift crust in West Antarctica (55 km) compared to East Antarctica (32 km), show that a necessary condition for broad rifting is a relatively warm uppermost mantle, with temperatures at the base of the crust >675 °C. At lower temperatures, a narrow rift behavior emerges in their models. Conversely, in order to retain high elevations in the Transantarctic Mountains, which they model as a stranded remnant of the collapsed Mesozoic plateau, uppermost mantle temperatures prior to rifting must be below ~850 °C. At higher temperatures, the lower crust beneath the Transantarctic Mountains becomes weak and flows laterally, preventing formation of an isostatic root beneath the mountains and inhibiting formation of the Transantarctic Mountain uplift.

Van Wijk et al. (2008) also examined a plateau collapse model, focusing on extension at the boundary between the stable East Antarctica craton and the postulated West Antarctica orogenic plateau. Like the Bialas et al. model, these models require a moderately warm temperature at the base of the crust (~750 °C) to produce wide rifting in the WARS. Also like the Bialas et al. models, their models show that the Transantarctic Mountains uplift may form as a remnant edge of the collapsed orogenic plateau, with the tectonic boundary between East and West Antarctica playing a key role in controlling the positions of rift localization in the Victoria Land Basin and the Transantarctic Mountains uplift.

Huerta and Harry (2007) developed a series of finite element models to investigate the cause of the transition from a broad extensional province in Late Cretaceous through Late Oligocene time to focused rifting within the Victoria Land Basin during Neogene time. In these models, West Antarctica prior to rifting is represented with a relatively thick crust but thin lithosphere in comparison to East Antarctica. These models show that the transition from a prolonged period of Cretaceous through Paleogene broad rifting to focused rifting during Neogene time may be a result of the thermal evolution of the WARS lithosphere and its pre-rift mechanical and thermal structure rather than a result of changes in plate boundary forces or basal boundary conditions. The thick crust beneath West Antarctica is the weakest part of the system prior to rifting, and so begins to extend first, forming the broad WARS extensional province. Cooling of the mantle during rifting strengthens the lithosphere. Eventually, the interior of the extending WARS becomes stronger than the unextended (and initially stronger) region between the WARS and the East Antarctic craton. The locus of extension then shifts westward, into the relatively narrow region where the lithosphere transitions between East and West Antarctica. Consistent with the results of Bialas et al. (2007) and van Wijk et al. (2008), the models of Huerta and Harry (2007) require temperatures at the base of the crust ranging from 680 to 780 °C in order to reproduce the tectonic evolution of the WARS. At lower temperatures, a narrow rift develops early, precluding

formation of the broad region of extension in the Ross Embayment. At higher temperatures, extension never localizes to form a narrow Neogene rift at the boundary between East and West Antarctica.

■ NEW MODEL CONSTRAINTS ON THE THERMAL EVOLUTION OF THE WARS

Purpose

The geodynamic models described above suggest that the evolution of the West Antarctic Rift System was sensitive to the pre-rift thermal state of the lithosphere. Here, we expand on the previous modeling studies to examine a larger parameter space in order to determine whether WARS-like rift behavior (the transition from broad extension to narrow rifting near the boundary between East and West Antarctica) can be achieved in models with plume-like mantle temperatures. The models shown here complement those of Huerta and Harry (2007) by examining a broader range of pre-rift temperature conditions in the lithosphere and asthenosphere and a broader range of thicknesses for the pre-rift WARS crust. We show that the transition from broad to focused rifting is a robust model behavior over a broad range of initial geometrical and thermal conditions. The position at which the narrow rift ultimately forms depends strongly on the initial thermal state of the lithosphere and upper mantle.

Model Setup and Variables

The modeling method is described in detail by Huerta and Harry (2007). The finite element method is used to solve the Stoke's equation to simulate incompressible viscoplastic flow in a rheologically layered lithosphere (Dunbar and Sawyer, 1989). The heat equation, including radiogenic heat production in the crust, is solved to track the thermal evolution of the model. Ductile deformation obeys a power law creep rheology that is dependent upon temperature and strain rate:

$$\varepsilon = A\sigma^n e^{-Q_c/RT},\qquad(1)$$

where A, n, and Q_c are physical properties depending on the lithology, T is temperature, and R is the Universal Gas Constant (Carter and Tsenn, 1987; Ranalli and Murphy, 1987). Flow laws for dunite and diorite are used for the crust and mantle, respectively. Plastic yielding at high stress is simulated by imposing a depth-dependent maximum stress according to Byerlee's law:

$$\sigma_{max} = C_0 + C_1 P_L,\qquad(2)$$

where P_L is lithostatic pressure, C_0 is the unconfined rock strength, and C_1 is a physical constant. Rheological and physical properties used in the models are given in Table 1. Constant extension rate and zero heat flux boundary conditions are applied at the sides of the models. Lithostatic stress and constant

TABLE 1. MODEL PARAMETERS

Thermal parameters	WARS crust	EA crust	Mantle
Thermal conductivity, W m^{-1} °C^{-1}	2.5	2.5	3.4
Specific heat, J kg^{-1} °C^{-1}	875	875	1250
Coefficient of thermal expansion, °C^{-1}	3.1×10^{-5}	3.1×10^{-5}	3.1×10^{-5}

Rheologic parameters	Crust	Mantle
Viscous rheology*		
A, s^{-1} Pa^{-n}	5×10^{-18}	4×10^{-25}
Q, kJ mol^{-1}	219	498
n	2.4	4.5
ρ, kg m^{-3}	2850	3300
Plastic rheology†		
S, MPa	60	60
B, MPa km^{-1}	11	11

Note: WARS—West Antarctic Rift System; EA—East Antarctica.

*$\sigma = [\varepsilon/A]^{1/n} e^{Q/nRT}$

†$\sigma = S + Bz$

temperature boundary conditions are applied at the base of the model. The models are started in thermal equilibrium.

The model setup is identical to that used by Huerta and Harry (2007) (Fig. 3). The East Antarctica structure is the same in all models, with a 39-km-thick crust and 180-km-thick lithosphere. West Antarctica has a thicker crust and thinner lithosphere prior to rifting (the thickness of both is varied between models). The eastern (Marie Byrd Land) side of the rift is not modeled. The thickness of the crust is tapered linearly across a 60-km-wide transition zone between East and West Antarctica. The base of the lithosphere is defined by an isotherm, with the temperature being a model variable. The depth of the isotherm, defining the pre-rift thickness of the lithosphere, is 180 km in East Antarctica and is a model variable in West Antarctica. The lithosphere thickness is tapered linearly across a 150-km-wide transition zone between the East and West Antarctica portions of the model. The edges of the regions of transitional crust and lithosphere thicknesses coincide on the West Antarctica side of the models, such that the transitional lithosphere extends further beneath the East Antarctic craton than the transitional crust. Assuming the lithosphere is in thermal equilibrium with the underlying mantle (not modeled), the initial temperature at the base of the model corresponds to the mantle potential temperature when adiabatically corrected to surface pressure.

Key parameters that were varied between different simulations are the thickness of the pre-rift WARS crust and lithosphere (ranging from 40 to 55 km and 150–200 km, respectively), the amount of heat generation in the crust (the product of the thickness of the heat producing layer and the rate of heat production, ranging from 37 to 93 mW m^{-2}), and the asthenosphere potential temperature T_p (the adiabatically corrected boundary condition at the bottom of the model) (Table 2). Model T_p ranges from 1240 °C (slightly

cooler than the global average) to 1367 °C (within the range suggested for a modest mantle plume). The model thermal properties combine to result in an initial mantle heat flux in West Antarctica ranging from 10 to 32 mW m^{-2}. The mesh geometry and time step size were chosen by testing selected models with progressively finer discretizations until successive models produced deformed meshes with a global root mean square difference in node positions at 50 m.y. of less than 100 m. The finer of the two discretizations in the model pair passing this test was used for all models. Additional model suites were examined (not shown here) to investigate the effects of varying the amount of heat generation in the East Antarctica lithosphere, the thickness of the East Antarctica lithosphere, the extension rate, and the widths of the regions in which the crust and lithosphere are tapered between East and West Antarctica. These parameters were found to affect the timing at which a lithospheric neck forms (marking the onset of narrow rifting development in the model), but they do not determine whether and where a lithospheric neck forms. All simulations were terminated when the crust in the necking region was thinned to less than 5 km.

■ RESULTS

Extensional Styles and Space-Time Trends

In all of the models, West Antarctica is laterally homogeneous and is initially weak in comparison to East Antarctica due to its thicker crust and warmer geotherm. Consequently, extension is initially broadly distributed throughout the WARS in all models. As extension progresses, the lithosphere is subject to

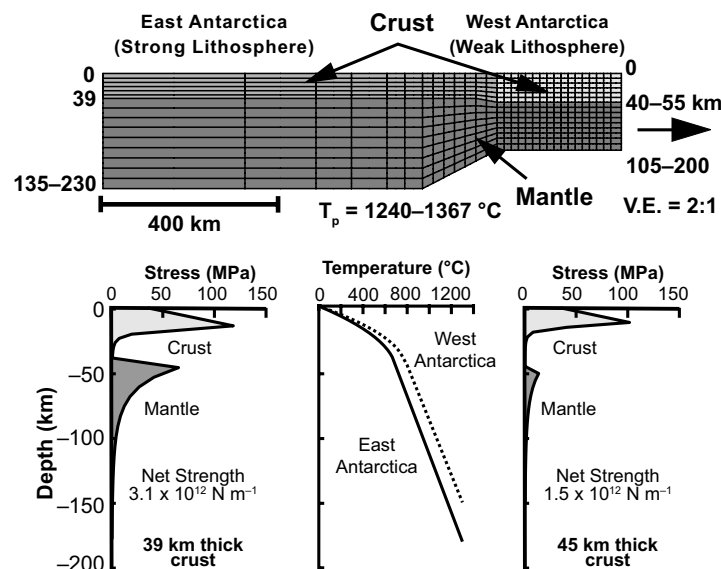Harry et al. | Geodynamic models of the West Antarctic Rift System

Figure 3. Finite element model mesh prior to extension. All models discussed in the text have similar starting geometry. The East Antarctica crust is 39 km thick in all models, and the pre-rift lithosphere is always thicker and the crust thinner in East Antarctica than in West Antarctica. The thicknesses of the crust and lithosphere are tapered over overlapping 60-km-wide and 150-km-wide transitional regions beginning 1050 km from the left (East Antarctica) edge of the model. Geometrical parameters varied between models are the thicknesses of the West Antarctica lithosphere (105–200 km) and West Antarctica crust (40–55 km). Thermal parameters varied between models are the temperature at the base of the lithosphere (ranging from 1300 to 1400 °C, equating to a mantle potential temperature ranging from 1240 to 1367 °C), the thickness of the radiogenic layer within the crust (30–45 km), and the volumetric crustal heat production rate ($1.4–3.1 \times 10^{-6}$ mW m^{-3}). A constant extension rate of 7 mm yr^{-1} is applied at the West Antarctica edge of the model (arrow) and lithostatic and adiabatic boundary conditions are applied at the bottom. Representative yield stress curves are shown for East Antarctica (lower left) and West Antarctica (lower right) prior to extension assuming a nominal strain rate of 10^{-15} s^{-1} and the temperature profile shown at bottom center. V.E.—vertical exaggeration.

the competing processes discussed previously: thinning, which mechanically weakens the lithosphere by decreasing the cross sectional area over which extensional stress is distributed; and cooling, which strengthens the lithosphere by increasing the strength of the ductile portion of the lithosphere (especially the uppermost mantle). These competing effects control the long-term behavior of the model, particularly where and when a lithospheric neck develops and whether the neck evolves into a narrow rift or whether it strengthens and is abandoned.

The models are differentiated into three classes on the basis of their necking behavior (Fig. 4). As noted above, all of the models begin with an initial period during which extension is distributed across the breadth of the pre-existing region of thicker crust in West Antarctica. Class 1 models continue in this way for more than 80 m.y., forming a broad extensional province that lacks a defined rift axis or lithospheric neck (Fig. 4A). With continued extension, Class 1 models ultimately develop a lithospheric neck at the edge of the model furthest from East Antarctica (Fig. 4B). Experimentation with wider models (additional columns added to the West Antarctica edge of the model) shows this to be a robust behavior. Wider Class 1 models take longer to neck, but all of them ultimately neck at the edge of the model furthest from East Antarctica. In Class 2 and Class 3 models, the initial period of broad extension lasts only 20–60 m.y., and is followed by a period of more focused lithospheric necking and formation of a narrow rift axis within the interior of the model. In Class 2 models, the neck forms within the interior of the broad extensional province (the region of initially thickest crust), resulting in a narrow central rift flanked by wide areas of previously extended crust (Fig. 4C). In Class 3 models, the neck forms at the western edge of the extensional province, in the region where the crust and lithosphere thicknesses were transitional between East and West Antarctica prior to rifting, and in a position coinciding with the modern location of the Victoria Land Basin (Fig. 4D). Class 3 models resemble the tectonic evolution of the WARS.

The models all have similar starting geometry and extension rate, with the primary differences being the pre-rift thicknesses of the West Antarctica crust and lithosphere, the temperature at the base of the lithosphere, and the rate of heat production and thickness of the heat producing layer in the West Antarctica crust. These variables control the pre-rift thermal state of the model lithosphere, which we characterize with the key parameters T_p (the mantle potential temperature, which is the temperature at the base of the lithosphere adiabatically corrected to surface pressure) and T_m (the temperature at the top of the mantle, which depends on T_p, and the rate and distribution of heat production in the crust). The models define a triangular shaped array in pre-rift T_p-T_m space (Fig. 5). The top (high T_m) boundary of the array results from limiting the models to those with lower crust temperatures below the solidus (~900 °C). The left and right boundaries of the array have positive slopes because increasing T_p leads to higher T_m, in general. Models outside these boundaries require that net crustal heat production be either unrealistically low (high T_p boundary) or unrealistically high (low T_p boundary), given the range of T_p examined here (discussed above). In this study we did not examine models with T_m <650 °C. Huerta and Harry (2007) found that models occupying this portion of the parameter space develop necks at the edge of the model furthest from East Antarctica (similar to the Class 1 models shown here) within the first 20–40 m.y. after the onset of extension (their class iii models).

TABLE 2. MODEL VARIABLES

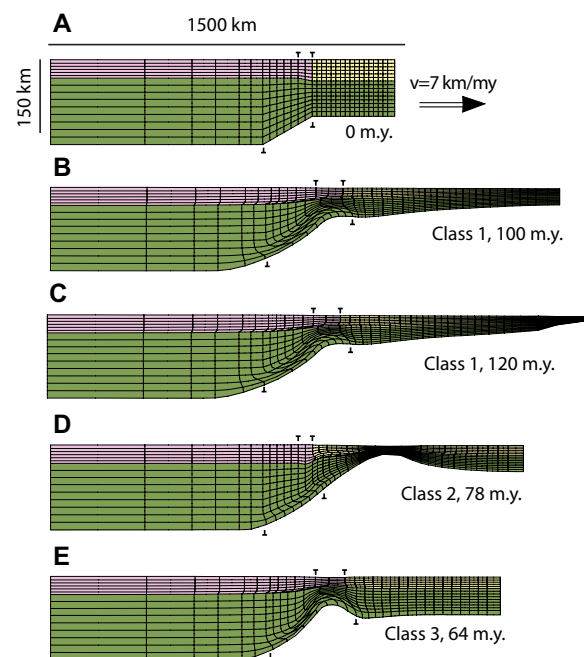| Variable	Range of investigation
Mantle potential temperature	1240–1380 °C
WARS crust heat generation	37–93 mW m^{-2}
WARS pre-rift crust thickness	40–55 km
WARS pre-rift lithosphere thickness	105–200 km

Note: WARS—West Antarctic Rift System.

Figure 4. Finite element model behaviors. (A) All models begin with a similar geometry, differing in initial thermal state and the thickness of the West Antarctica crust and mantle. (B) Class 1 models (dominant behavior)—deformation is uniformly distributed throughout West Antarctica, forming a broad extensional province lasting for ca. 100 m.y. (C) Class 1 models (late behavior)—continued extension leads to abrupt formation of a lithospheric neck and narrow rift at the edge of the model furthest from East Antarctica. (D) Class 2 models (late behavior)—a lithospheric neck develops within the interior of West Antarctica after an initial period of broad extension in West Antarctica. (E) Class 3 models (late behavior)—a lithospheric neck develops near the East Antarctica/West Antarctica boundary after a period of broad extension in West Antarctica. Crossed bars indicate the edges of the transition zone between cratonic East Antarctica and the thermally more juvenile lithosphere of West Antarctica.

Figure 5. Model behavior as a function of temperature at the base of the crust (T_m) and asthenosphere potential temperature (T_p) at intervals of 20 m.y. after the onset of extension. Symbols indicate the style of extension of each model at the times noted: uniform broad extension throughout West Antarctic Rift System (WARS) (gray squares), necking at the edge of the model (red asterisks), necking within the WARS interior (blue crosses), necking within the transition zone between East and West Antarctica (green crosses). Model parameter space is bounded by regions requiring unrealistically low crustal heat production (Q_c) if a given T_m is to be maintained at higher T_p (right boundary), unrealistically high Q_c if a higher T_m is to be achieved with a given T_p (left boundary), and lower crust temperatures approaching the solidus (top boundary). Overlap between model behaviors within the parameter space results primarily from differences in how heat generation in the crust is partitioned between volumetric heat production and the thickness of the heat producing layer. Dashed box indicates parameter space occupied by class iii models of Huerta and Harry (2007) that developed necks at the West Antarctica edge of the model within 40 m.y. after the onset of extension. The style of extension at 120 m.y. is used to define the model classes discussed in the text.

Different necking behaviors over time are associated with specific areas in the model T_p-T_m parameter space (Fig. 5). Overlap between these regions is relatively minor, and is due to small variations in the pre-rift thickness of the crust, the volumetric rate of heat production, and the thickness of the heat producing layer. All of the models have broadly distributed extension during the first ca. 20 m.y., and transition from broad to focused rifting within 120 m.y. The time at which the rift neck forms differs between the various model classes. Necks first appear in Class 2 and 3 models 20 m.y. after the onset of extension. Most develop lithospheric necks within 60 m.y., and all models displaying these types of necking behaviors develop necks within 80 m.y.
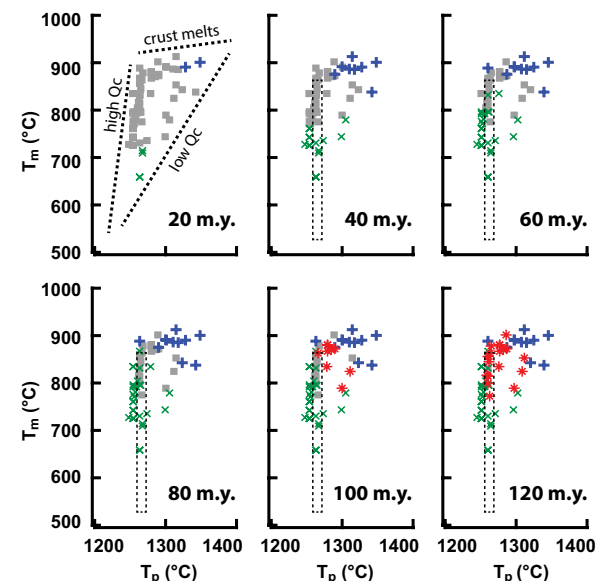
after the onset of extension. In contrast, the Class 1 models do not begin to develop necks until 100 m.y. after the onset of extension. The Class 3 models that develop necks earliest have relatively low temperatures at the base of the crust (T_m <780 °C) and base of the lithosphere (T_p <1300 °C) and relatively low surface heat flux (Q_s <75 mW m^{-2}, not shown). The Class 2 models that develop necks earliest lie at nearly the opposite end of the model parameter space from Class 3 models, with moderately high mantle potential temperatures (T_p >1300 °C), high temperatures at the base of the crust (T_m >850 °C), and higher surface heat flow (Q_s >77 mW m^{-2}). Class 1 models occupy the intervening parameter space.
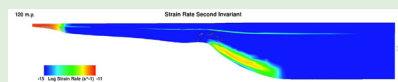
Model Class 1—Broad Extension within the WARS Culminating in Neck at Edge of Model

In Class 1 models, deformation is broadly distributed across West Antarctica for ca. 80 m.y. or more before focusing at the edge of the model (Fig. 6; Supplemental Animation 1[1]). All of the Class 1 models have relatively high temperatures at the top of the mantle (T_m >780 °C) (Fig. 5). In some models this is due to relatively high asthenosphere temperatures and/or a thin lithosphere,
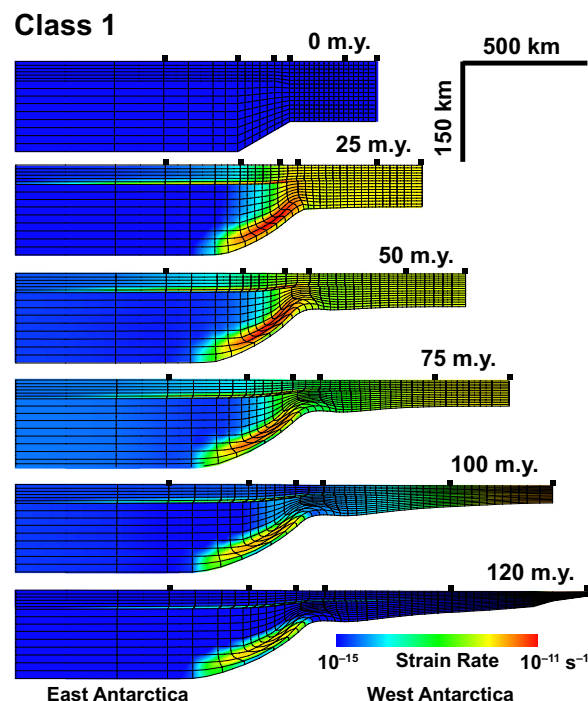

Class 1

0 m.y.

500 km

150 km

25 m.y.

50 m.y.

75 m.y.

100 m.y.

120 m.y.

10^{-15} **Strain Rate** 10^{-11} s^{-1}

East Antarctica   **West Antarctica**

Figure 6. Typical Class 1 model showing second invariant of the strain rate. Black lines indicate finite element mesh. Squares at top of mesh indicate reference positions shown in Figures 7 and 8. From left to right: P_{EAI}, P_{TZE}, P_{TZI}, P_{TZW}, P_{WAI}, and P_{WAE}. Moderately high strain rate is broadly distributed throughout West Antarctica for the first 100 m.y. of extension. By 120 m.y. extension has become strongly focused within a narrow rift at the edge of the model furthest from East Antarctica. Minor extensional strain extending into the East Antarctica crust during the first 75 m.y. in this model is decoupled from the underlying unstrained mantle by a detachment at the base of the crust (narrow layer of high strain rates). High strain rates at the base of the lithosphere near the center of the model result from flow of the lowermost lithosphere mantle, away from the transitional lithosphere separating East and West Antarctica and into the extending West Antarctic Rift System region. The simulation was terminated at 120 m.y. when the crust in the necking region had thinned to less than 5 km. See Supplemental Animation 1 [text footnote 1].

whereas in other models this is due to relatively high heat production in the crust. The warm upper mantle results in a substantially weaker pre-rift West Antarctica lithosphere in comparison to East Antarctica, causing broad extension throughout the WARS and in the transition zone between the WARS and East Antarctica during the early stages of extension.

In the following, we discuss the behavior of the Class 1 model shown in Figure 6 in the context of feedbacks between changes in the thickness of the crust (and the stretching factor β, which is the ratio of crust thickness before and after extension), the temperature of the uppermost mantle, and the net strength of the lithosphere as a function of time (t) and horizontal position (x). The net strength of the lithosphere is calculated at each time and each horizontal position in the model by integrating the yield stress over the thickness of the lithosphere. The yield stress as a function of depth is computed using the model thermal and rheological structures and assuming a constant strain rate of 10^{-15} s^{-1}. We focus specifically on the evolution of the model at six locations: position P_{WAE}, at the West Antarctica edge of the model; P_{WAI}, near the center of the extending WARS province; P_{TZW}, at the West Antarctica edge of the region where the pre-rift crust and lithosphere thicknesses are transitional between East and West Antarctica (hereafter referred to as the transitional region or transitional lithosphere); P_{TZI}, in the interior of the region of transitional lithosphere; P_{TZE}, at the East Antarctica edge of the region of transitional lithosphere; and P_{EAI}, in the interior of East Antarctica.

The strength of the lithosphere in West Antarctic resides primarily within the crust during the first ca. 50 m.y. of extension (Fig. 7A, 7B). As extension progresses, the uppermost mantle cools and becomes progressively stronger, becoming the strongest part of the WARS lithosphere by 70 m.y. The net strength of the WARS lithosphere decreases during this time (Fig. 7G), indicating that mechanical weakening due to thinning of the lithosphere dominates over thermal strengthening due to cooling in the WARS. The uppermost mantle in the transitional region between East and West Antarctica is initially moderately stronger than in West Antarctica (and becomes progressively stronger from east to west) (Figs. 7C, 7D). The mantle becomes stronger with time in this region (due to cooling), as in the WARS, but the lithosphere undergoes less thinning (because the transitional region has greater strength than West Antarctica). As a consequence, the net strength of the lithosphere within the transitional region increases with time (Fig. 7G). The uppermost mantle in East Antarctica is initially much stronger than in West Antarctica and in the transitional region, resulting in a much larger net strength (Figs. 7E, 7F). Consequently, East Antarctic undergoes little extension and retains its pre-rift thermal structure and strength throughout the duration of the model simulation (Fig. 7G).

Extension and crustal thinning are uniformly distributed across the breadth of West Antarctica during the first 70 m.y. of extension, forming a broad extensional province analogous to the WARS (Figs. 6, 8A, and 8B, note parallel contours showing similar amounts of thinning over the breadth of the West Antarctica portion of the model and the nearly parallel trajectories of the West Antarctica reference positions P_{WAE} and P_{WAI} indicating similar amounts and rates of thinning at different positions within the WARS). Thinning in this
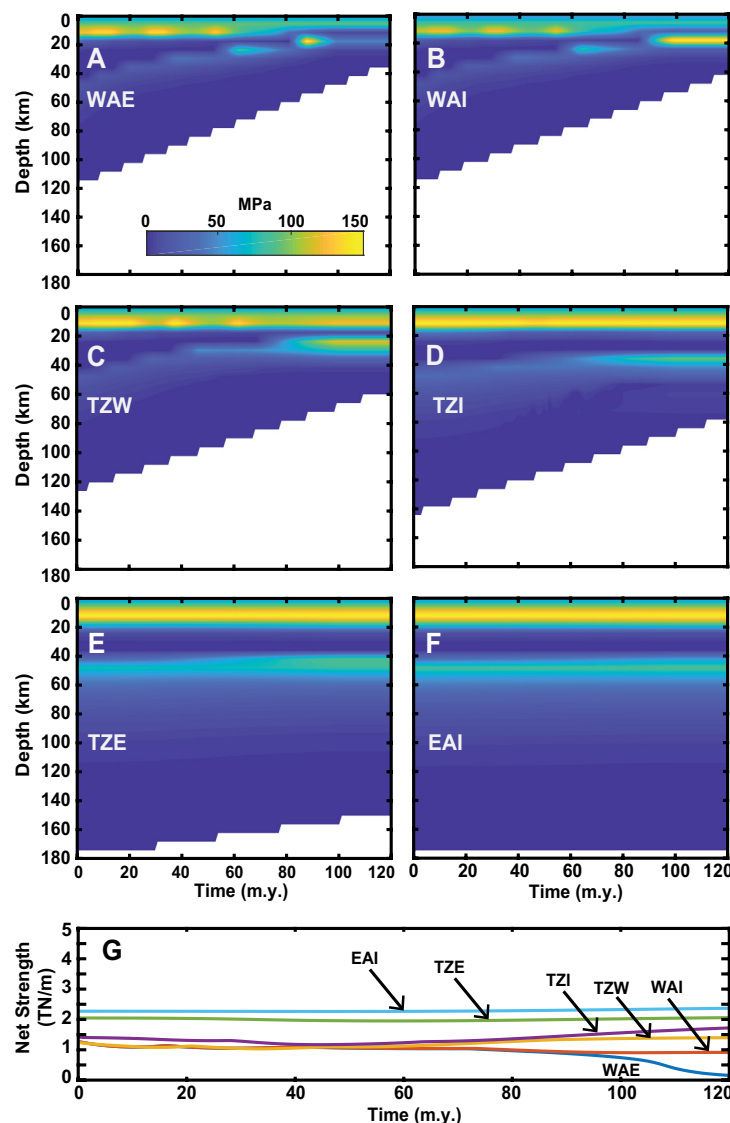
Figure 7. Yield stress for Class 1 model as a function of depth and time at selected horizontal positions. Model is shown in Figure 6. Yield stress is computed using the model temperature and rheological structure and a constant strain rate of 10^{-15} s^{-1}. (A) Position P$_{WAE}$, at the West Antarctica edge of the model. (B) P$_{WAI}$, in the interior of the West Antarctic Rift System. (C) P$_{TZW}$, at the West Antarctica edge of the region of transitional lithosphere between East and West Antarctica. (D) P$_{TZI}$, in the interior of the region of transitional lithosphere. (E) P$_{TZE}$, at the East Antarctica edge of the region of transitional lithosphere. (F) P$_{EAI}$, in the interior of East Antarctica. (G) Net strength of the lithosphere for each position (the vertical integral of A–F).

region is relatively rapid during the first 20 m.y. and becomes progressively slower between 20 and 70 m.y. as the WARS widens (Fig. 8A, note closely spaced crust thickness contours prior to 20 m.y. and increasingly wider spacing afterward). Rapid thinning (promoting mechanical weakening) and minimal cooling (inhibiting thermal strengthening, Fig. 8C) combine to result in a decrease in the strength of the WARS lithosphere during the first 20 m.y. of extension (Fig. 8D, note P$_{WAE}$ and P$_{WAI}$ trajectories crossing lithosphere strength contours). The strength of the lithosphere in most of the WARS region is relatively constant between 20 and 70 m.y., indicating that mechanical weakening due to thinning of the WARS lithosphere during this time is approximately balanced by thermal strengthening as the uppermost mantle cools.

The uppermost mantle in the westernmost WARS is cooler than in the interior of the WARS during the first 20 m.y. of extension (Fig. 8C, note small westward decrease in upper mantle temperature between reference positions P$_{WAI}$ and P$_{TZW}$). This is due to its proximity to the cooler East Antarctica lithosphere. Because it is initially cooler (and hence stronger) than the rest of the WARS (Figs. 8C, 8D), the part of West Antarctica adjacent to the transitional lithosphere undergoes less extension. This forms a narrow region of anomalously thick crust in the western WARS that becomes progressively more pronounced between 20 and 70 m.y. (Fig. 8A, between reference positions P$_{WAI}$ and P$_{TZW}$).

The western part of the transitional region differs from East Antarctica only in that the depth to the bottom of the model lithosphere (defined by the model's basal isotherm) decreases eastward, resulting in sharp horizontal gradients in mantle temperature and lithospheric strength prior to extension (Figs. 8C, 8D). This area evolves similarly to East Antarctica, undergoing little thinning and thus retaining close to its pre-rift thermal structure and strength (Figs. 7 and 8G, note trajectories of reference positions P$_{TZI}$ and P$_{TZE}$). The eastern part of the transitional region is an area where the pre-rift thickness of both the crust and lithosphere change (the lithosphere thickness decreasing eastward as the crust thickness increases). This results in correspondingly sharp horizontal gradients in the uppermost mantle temperature, net strength of the lithosphere, and amount of crustal stretching in this region (Figs. 8B–8D). The central part of the region of transitional lithosphere, positioned between initially cooler East Antarctica and extending and cooling West Antarctica, becomes the warmest part of the upper mantle after ca. 2 m.y. (Fig. 8C).

The difference in the amount of stretching between the eastern and western WARS creates a gradient in the net strength of the lithosphere that dominates the model behavior after 70 m.y. (Fig. 8D). The strength gradient (a result of the initial temperature gradient caused by juxtaposition of West Antarctica against cooler East Antarctica) promotes more rapid extension toward the eastern edge of the model. This, in turn, leads to more rapid mechanical weakening, causing extension to become progressively more focused toward the West Antarctica edge of the model (Fig. 8A, note trajectories of reference positions P$_{TZW}$ and P$_{WAI}$ become parallel to crust thickness and β contours, indicating a cessation of thinning in these areas, at successively later times after 70 m.y.). The western WARS and the region of transitional lithosphere cool and strengthen slightly as extension wanes in these areas (Figs. 8C, 8D).
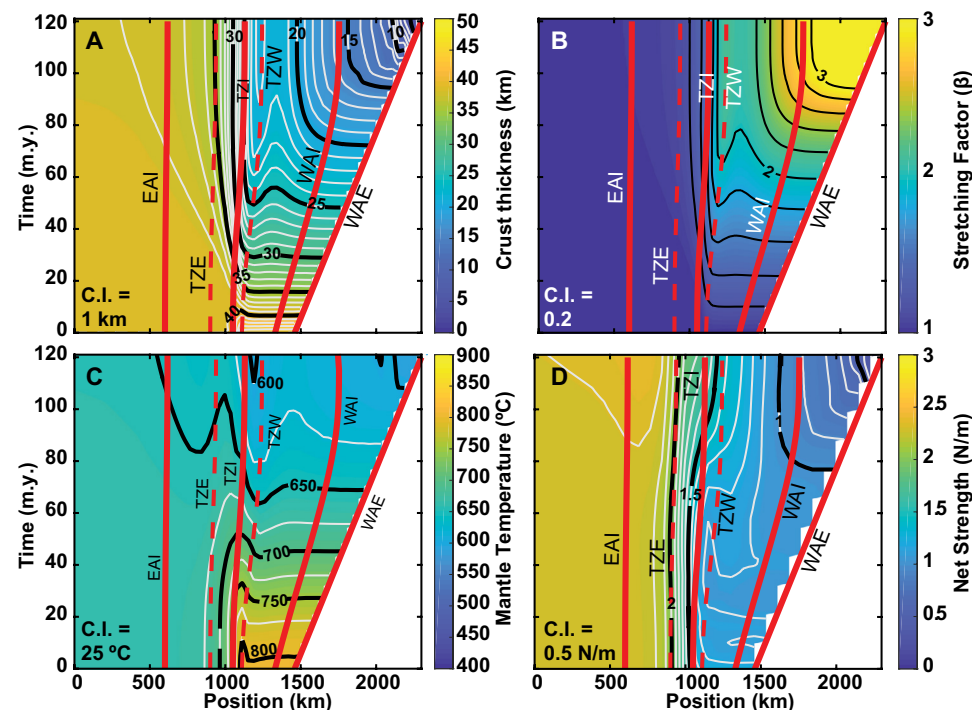
Figure 8. Typical Class 1 model thermal and mechanical evolution. Model is shown in Figure 6. (A) Thickness of the crust. (B) Stretching factor β. (C) Temperature at the top of the mantle. (D) Net strength of the lithosphere. Solid red lines show positions through time of reference points located at the West Antarctica edge of the model (P_{WAE}), within the interior of West Antarctica (P_{WAI}), in the middle of the region where the pre-rift crust and lithosphere thicknesses are transitional between East and West Antarctica (P_{TZI}), and within the interior of East Antarctica (P_{EAI}). Dashed red lines mark the boundaries of the region with transitional pre-rift lithosphere (P_{TZW} on the eastern, or West Antarctica side, and P_{TZE} on the western, or East Antarctica side). C.I.—contour interval.

The behavior described above is common to all Class 1 models. The temperature difference between East and West Antarctica results in an initial period of uniform broad extension in the WARS region. A temperature gradient in the upper mantle across the WARS, caused by its juxtaposition against cooler East Antarctica on one side, produces a horizontal strength gradient that ultimately leads to progressive focusing of extension at the West Antarctica edge of the model. The timing of the transition from broadly distributed extension to progressively more focused extension varies between Class 1 models depending on the initial temperature difference between East and West Antarctica, the initial thickness of the West Antarctica crust and lithosphere, and the steepness of the crust and lithosphere thickness gradients in the transitional lithosphere between East and West Antarctica.

Model Class 2—Necking within the Interior of West Antarctica

Class 2 models initially behave similarly to the Class 1 models, beginning with a period of broadly distributed extension that is followed by a transition to narrow rifting (Fig. 9; Supplemental Animation 2 [footnote 1]). In Class 2 models, the lithospheric neck develops within the interior of West Antarctica,

in the central part of the region of thickened crust, rather than near the model edge as in the Class 1 models.

The East Antarctica lithosphere is much cooler in the Class 2 models than in the Class 1 models, and the West Antarctica lithosphere is warmer and thus weaker. As a result, the strength gradient across the region of transitional lithosphere and the difference in net strength of the lithosphere between East and West Antarctica is much more pronounced (Figs. 10, 11C and 11D). As in the Class 1 models, the upper mantle at the western edge of the model is initially weak, and becomes stronger with time (Fig. 10A). The upper mantle in the central WARS also is initially weak, but unlike the Class 1 models and the western edge of the Class 2 models, the central WARS upper mantle remains relatively weak throughout the duration of the model simulation (Fig. 10B). The transitional lithosphere, like the East Antarctic lithosphere, has a relatively strong upper mantle in comparison to West Antarctica (Figs. 10C, 10D) and is thus minimally involved during extension (Figs. 11A, 11B). Consequently, it retains nearly its initial thermal and strength structure throughout the duration of the model simulation (Figs. 10G, 11C, and 11D).

The period of broadly distributed extension in the Class 2 models evolves similarly to the Class 1 models, beginning with a ca. 15 m.y. (in the model shown here) period of rapid thinning of the lithosphere that is accompanied by

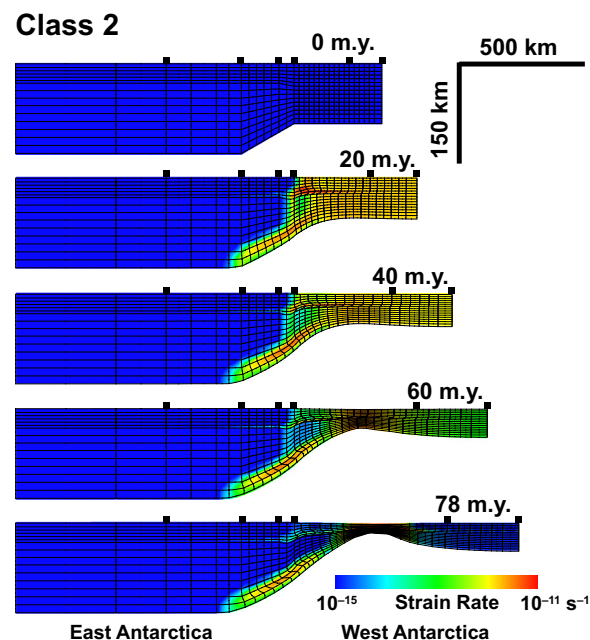Harry et al. | Geodynamic models of the West Antarctic Rift System

Figure 9. Typical Class 2 model showing second invariant of the strain rate. Black lines indicate finite element mesh. Squares at top of mesh indicate reference positions shown in Figures 10 and 11. From left to right: P_{EAI}, P_{TZE}, P_{TZI}, P_{TZW}, P_{WAI}, and P_{WAE}. Moderately high strain rate is initially broadly distributed throughout West Antarctica. Extension becomes more focused and a narrow rift develops within the interior of West Antarctica after 60 m.y. High strain rates at the base of the lithosphere near the center of the model result from flow of the lowermost lithosphere mantle into the extending West Antarctic Rift System region and away from the region of transitional lithosphere separating East and West Antarctica. The simulation was terminated at 78 m.y. when the crust in the necking region had thinned to less than 5 km. See animation in Supplemental Animation 2 [text footnote 1].

minimal cooling (Fig. 11). The net strength of the WARS lithosphere decreases slightly during this time (Fig. 11D). This period of syn-extensional weakening of the WARS lithosphere is followed by a period of decelerating cooling between 15 and 40 m.y. as the rate of thinning in the WARS decreases (Fig. 10C, note change in contour spacing after 15 m.y.).

Focusing of strain during the later stages of extension in the Class 2 models is due to the same processes as in the Class 1 models. Horizontal temperature and strength gradients develop in the Class 2 models as a result of juxtaposition of the warm West Antarctica lithosphere against cooler East Antarctica (Figs. 11C, 11D). This promotes progressive focusing of extension toward the east, away from the cooler and stronger part of the WARS that is adjacent to East Antarctica, beginning ca. 40 m.y. (Figs. 11A, 11B). The primary difference between Class 1 and Class 2 models is that thermal strengthening dominates
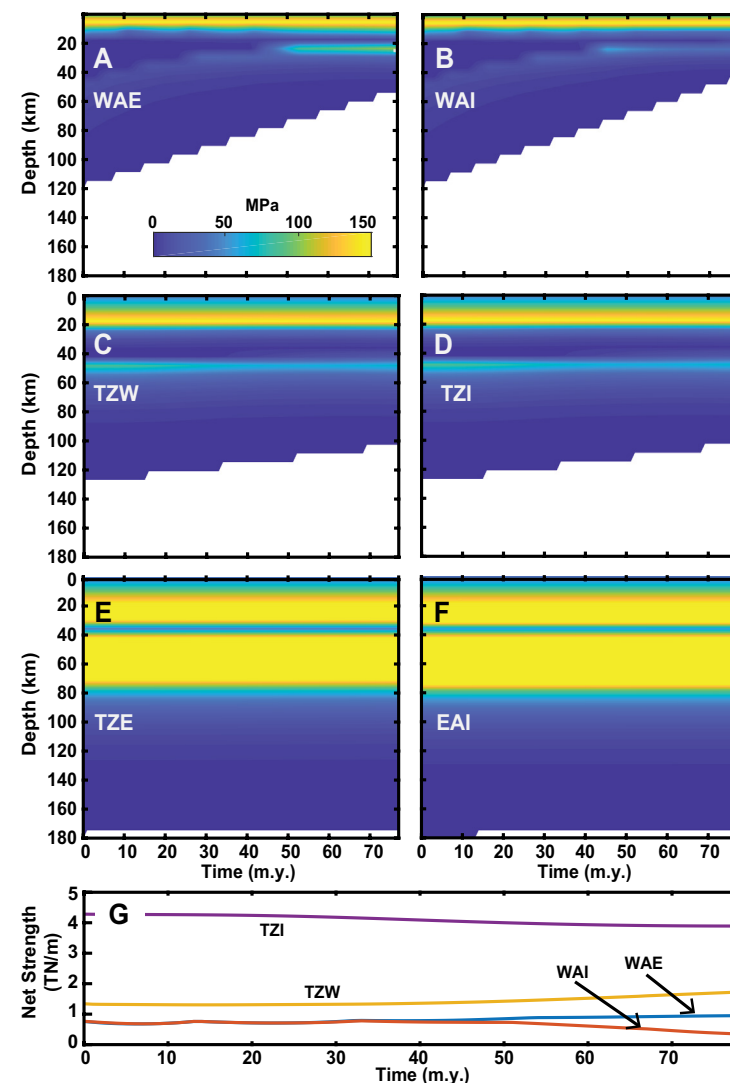

Figure 10. Yield stress for Class 2 model as a function of depth and time at selected horizontal positions. Model is shown in Figure 9. Yield stress is computed using the model temperature and rheological structure and a constant strain rate of 10^{-15} s^{-1}. (A) Position P_{WAE}, at the West Antarctica edge of the model. (B) P_{WAI}, in the interior of the West Antarctic Rift System. (C) P_{TZW}, at the West Antarctica edge of the region of transitional lithosphere between East and West Antarctica. (D) P_{TZI}, in the interior of the region of transitional lithosphere. (E) P_{TZE}, at the East Antarctica edge of the region of transitional lithosphere. (F) P_{EAI}, in the interior of East Antarctica. (G) Net strength of the lithosphere for each position (the vertical integral of A–F). The net strength of East Antarctica and the eastern transitional region (reference positions EAI and TZE) are greater than 12 TN/m, and are not shown on this figure.
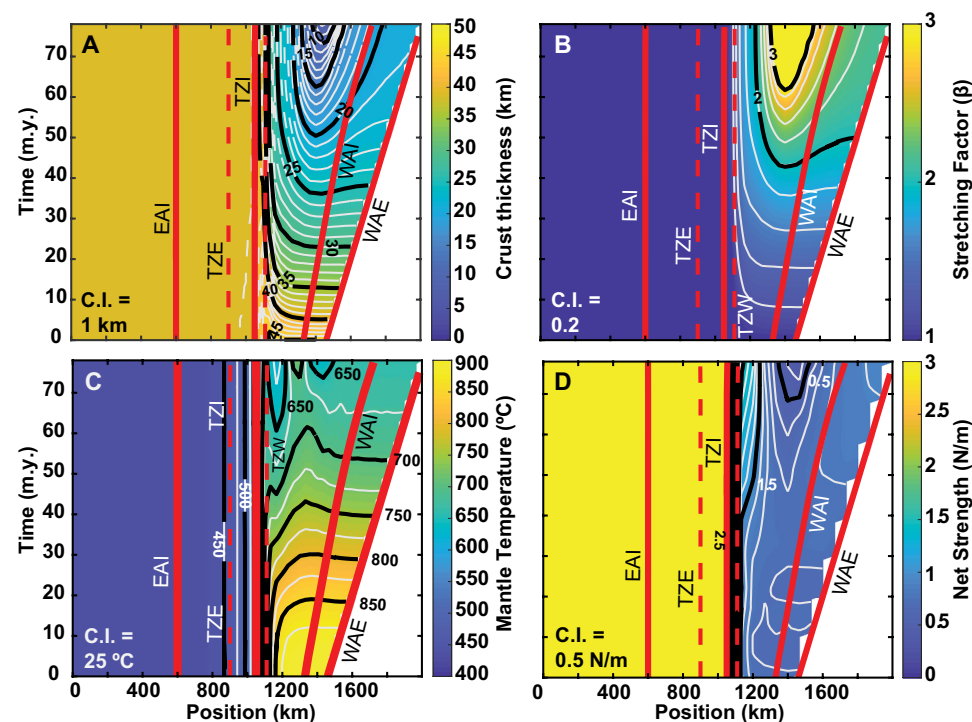
Figure 11. Typical Class 2 model thermal and mechanical evolution. Model is shown in Figure 9. (A) Thickness of the crust. (B) Stretching factor β. (C) Temperature at the top of the mantle. (D) Net strength of the lithosphere. Solid red lines show positions through time of reference points located at the West Antarctica edge of the model (P_{WAE}), within the interior of West Antarctica (P_{WAI}), in the middle of the region where the pre-rift crust and lithosphere thicknesses are transitional between East and West Antarctica (P_{TZI}), and within the interior of East Antarctica (P_{EAI}). Dashed red lines mark the boundaries of the region with transitional pre-rift lithosphere (P_{TZW} on the eastern, or West Antarctica side, and P_{TZE} on the western, or East Antarctica side). C.I.—contour interval.

at the eastern edge of the rift in the Class 2 models, whereas mechanical weakening dominates in the Class 1 models. In Class 2 models, the eastern edge of the model is able to cool sufficiently during extension to eventually become stronger than the less extended interior part of the WARS (at ca. 40 m.y. in the model shown here). This is because the crustal heat production is greater in the Class 2 models, and so thinning of the crust has a greater impact on the upper mantle temperature. As the lithosphere becomes dynamically (thermally) strengthened at the edge of the model and in the western WARS, deformation becomes constrained to the interior of the WARS. Because strain is focused in a relatively narrow region, lithosphere thinning is relatively rapid, permitting only minimal cooling. This further (mechanically) weakens the lithosphere (Fig. 10G) and leads progressively to formation of a lithospheric neck and narrow rift axis in the central WARS.

Model Class 3—Necking near the East Antarctica/West Antarctica Boundary

As in the Class 1 and Class 2 models, the Class 3 models initially undergo a period of broadly distributed extension followed by a transition to more focused extension and ultimately formation of a narrow lithospheric neck

(Fig. 12; Supplemental Animation 3 [footnote 1]). In Class 3 models, the lithospheric neck forms within the transition zone between East and West Antarctica. Class 3 models correspond to the class i models of Huerta and Harry (2007), and most closely resemble the evolution of the WARS, where broad extension was followed by narrow rifting near the East Antarctic flank of the rift.

The strength of the lithosphere in the Class 3 models evolves similarly to the Class 1 models. The upper mantle is initially weak beneath West Antarctica and begins to strengthen ca. 30 m.y. (in the model shown here) after extension begins (Figs. 13A, 13B). Unlike the class 1 models, the West Antarctica lithosphere is initially too thick to result in substantial mechanical weakening in this region. Thermal strengthening of the lithosphere dominates over mechanical weakening, and the net strength of the WARS lithosphere increases with time (Fig. 13G, positions P_{WAE} and P_{WAI}). The strength of the upper mantle changes significantly across the region of transitional lithosphere (Figs. 13C–13E). The upper mantle in the eastern part of the transitional region is initially weak, and strengthens with time, although not as much as in the WARS. The strength of the upper mantle in the western part of the transitional region lies between that of the eastern transitional region and East Antarctica, and strengthens only slightly with time. Thinning of the lithosphere and crust is more pronounced in the eastern transitional region in the Class 3 models than in the Class 1 and
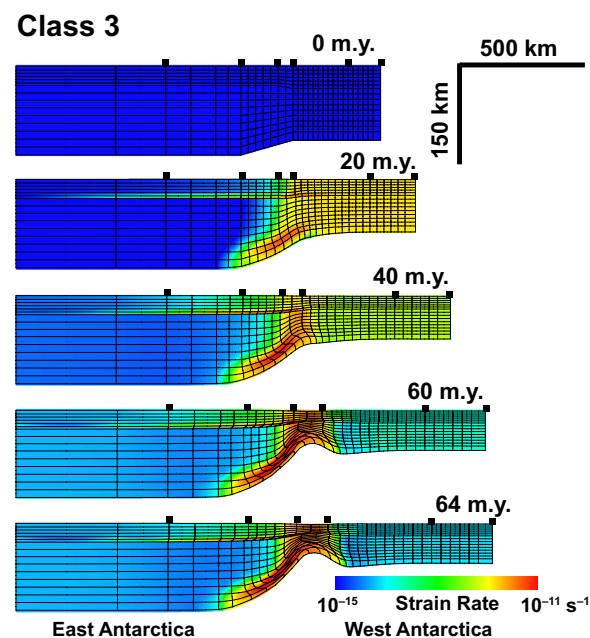
Figure 12. Typical Class 3 model showing second invariant of the strain rate. Black lines indicate finite element mesh. Squares at top of mesh indicate reference positions shown in Figures 13 and 14. From left to right: P_{EAI}, P_{TZE}, P_{TZI}, P_{TZW}, P_{WAI}, and P_{WAE}. Moderately high strain rate is initially broadly distributed throughout West Antarctica. Extension becomes more focused and a narrow rift develops in the transition zone between East and West Antarctica by 60 m.y. Minor extensional strain extends into East Antarctica in this model, with a detachment at the base of the crust (narrow layer of high strain rates) decoupling deformation in the crust and mantle. High strain rates at the base of the lithosphere near the center of the model result from flow of the lowermost lithosphere mantle into the extending West Antarctic Rift System region and away from the region of transitional lithosphere separating East and West Antarctica. The simulation was terminated at 64 m.y. when the crust in the necking region had thinned to less than 5 km. See animation in Supplemental Animation 3 [text footnote 1].

Class 2 models. As a result, mechanical weakening outpaces thermal strengthening, causing the net strength of the lithosphere in the transitional region to decrease with time in Class 3 models (Fig. 13, position P_{TZI}). The upper mantle and net strength of the East Antarctica lithosphere is strong at the onset of extension, due to the relatively thick and cool lithosphere in Class 3 models, and is little affected by extension (Figs. 13E–13G).

The initial period of broad rifting in the Class 3 models evolves similarly to the other models, with an early phase of rapid thinning and mechanical weakening of the lithosphere that involves minimal cooling (Fig. 14, between 0 and 10 m.y. in the model shown). This is followed by progressively decelerating
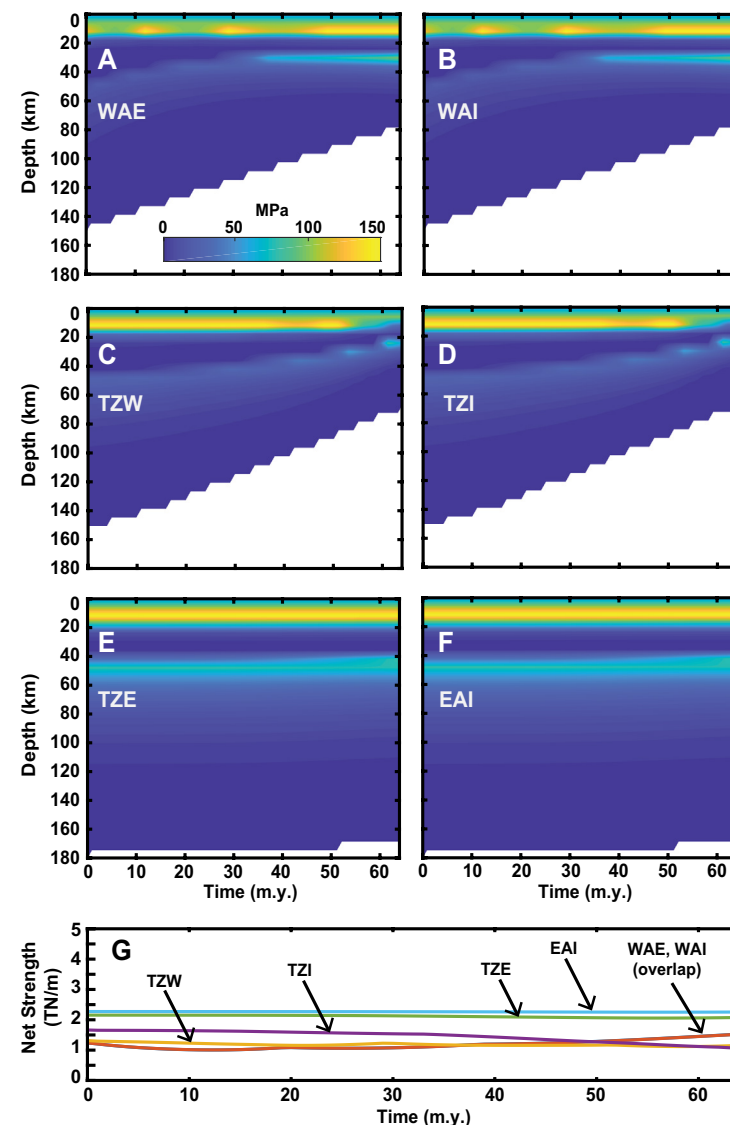

Figure 13. Yield stress for Class 3 model as a function of depth and time at selected horizontal positions. Model is shown in Figure 12. Yield stress is computed using the model temperature and rheological structure and a constant strain rate of 10^{-15} s^{-1}. (A) Position P_{WAE}, at the West Antarctica edge of the model. (B) P_{WAI}, in the interior of the West Antarctic Rift System. (C) P_{TZW}, at the West Antarctica edge of the region of transitional lithosphere between East and West Antarctica. (D) P_{TZI}, in the interior of the region of transitional lithosphere. (E) P_{TZE}, at the East Antarctica edge of the region of transitional lithosphere. (F) P_{EAI}, in the interior of East Antarctica. (G) Net strength of the lithosphere for each position (the vertical integral of A–F).
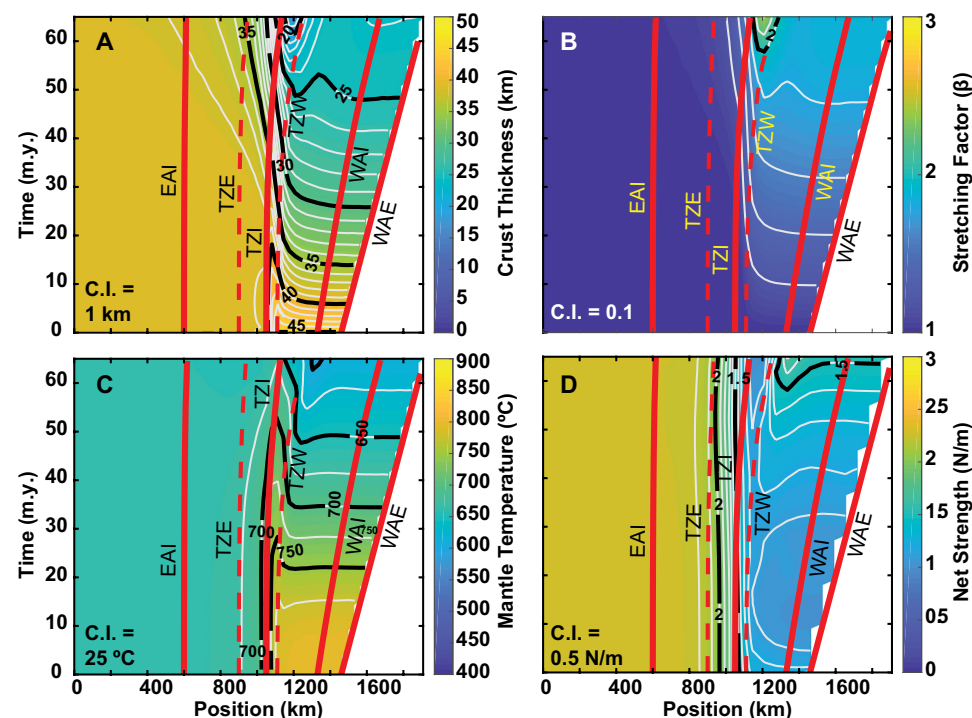
Figure 14. Typical Class 3 model thermal and mechanical evolution. Model is shown in Figure 12. (A) Thickness of the crust. (B) Stretching factor β. (C) Temperature at the top of the mantle. (D) Net strength of the lithosphere. Solid red lines show positions through time of reference points located at the West Antarctica edge of the model (P_{WAE}), within the interior of West Antarctica (P_{WAI}), in the middle of the region where the pre-rift crust and lithosphere thicknesses are transitional between East and West Antarctica (P_{TZI}), and within the interior of East Antarctica (P_{EAI}). Dashed red lines mark the boundaries of the region with transitional pre-rift lithosphere (P_{TZW} on the eastern, or West Antarctica side, and P_{TZE} on the western, or East Antarctica side). C.I.—contour interval.

thinning and more rapid cooling of the WARS lithosphere (from 20 to 30 m.y. in the model shown). The net strength of the lithosphere in the WARS is relatively stable during this period (Fig. 14D). Beginning at ca. 30 m.y., the rate of crustal thinning in the interior of the WARS begins to decrease and the lithosphere begins to cool more rapidly (Figs. 14A–14C). Thermal strengthening begins to dominate over mechanical weakening, and the net strength of the WARS lithosphere begins to increase (Figs. 13G and 14D). As the interior of the WARS becomes stronger, extension focuses in the now relatively weaker eastern part of the region of transitional lithosphere between East and West Antarctica. Once strain begins to focus, mechanical weakening dominates over thermal strengthening (Fig. 13G, position P_{TZI}), as in the Class 1 and Class 2 models, leading to rapid formation of a narrow rift in the eastern part of the transitional region (Fig. 14).

The cause for necking in Class 3 models is similar to that in Class 2 models. As the heat-producing layer in the West Antarctica crust thins during the early stages of rifting, the uppermost mantle cools and becomes stronger. In Class 2 models, this is most pronounced at the model's edge, causing extension to shift to a position in the interior of the WARS between the dynamically strengthening edge of the model and the stronger transitional lithosphere between East and West Antarctica. In Class 3 models, the difference in strength between the

transitional lithosphere and West Antarctica is not as large as in the Class 2 models. This allows the cooling and dynamically strengthening interior of the WARS to eventually become stronger than the as yet un-extended transitional lithosphere. Once this transition in strength occurs, deformation begins to focus in the now-weaker narrow transitional region, creating a narrow rift near the boundary between East and West Antarctica (e.g., Huerta and Harry, 2007).

The Class 3 models mimic in general terms the evolution of the WARS, with an initial period of broad rifting followed by formation of a narrow rift near the East Antarctica/West Antarctica boundary. All but two of the Class 3 models have a mantle potential temperature equal to or below 1280 °C, and none have a mantle potential temperature above 1310 °C (Fig. 5).

■ DISCUSSION

Discussion of Model Behaviors

Necking in the models is initiated by lateral gradients in the strength of the lithosphere, which produce stress gradients that focus strain. High temperatures minimize variations in strength, and thus inhibit focusing of extension

and formation of narrow rifts. If the upper mantle is very hot and remains hot during extension, lateral variations in strength remain minimal during extension. Lateral stress gradients are then subdued, strain localization is inhibited, and formation of a broad extensional province is favored (model Class 1, Figs. 5–8). At lower mantle potential temperatures, lateral strength variations in the uppermost mantle are more pronounced, producing stress gradients that promote strain focusing and ultimate formation of a narrow rift. The position at which the narrow rift axis forms depends on the thermal evolution of the lithosphere within the WARS and within the region of transitional crust and lithosphere thickness between the WARS and East Antarctica (model Classes 2 and 3, Figs. 9–14).

Juxtaposition of the warm West Antarctica lithosphere against the cooler East Antarctica craton creates a small horizontal temperature gradient that is initially present across West Antarctica in all of the models. The horizontal temperature gradient has a relatively small influence on the behavior of the rift during the early stages of extension when temperatures are high enough to inhibit strain localization. As extension progresses and the mantle cools, the lateral variation in strength produced by the temperature gradient begins to influence the rift behavior and strain begins to progressively focus toward the warmer edge of the model furthest from East Antarctica. This occurs between 20 and 80 m.y. in the models examined here. The necking behavior after the end of the initial period of broad extension in the models depends on whether strengthening of the lithosphere due to cooling (thermal strengthening) dominates over weakening of the lithosphere due to thinning (mechanical weakening) at the edge of the model.

In Class 1 models (Figs. 6–8), cooling of the WARS lithosphere is limited during extension and mechanical weakening at the edge of the model dominates the rift evolution. Because cooling is limited, the broad phase of extension is protracted, lasting more than 80 m.y. After the initial phase of broad extension the geotherm within the WARS stabilizes, and the lateral temperature gradient becomes the dominant cause of strength variations in the lithosphere. Thinning becomes slightly more rapid at the model edge due to its slightly higher temperature and correspondingly lower strength. Stress at the edge of the model then becomes more concentrated, promoting more rapid strain and leading to progressively and relatively rapidly focusing of deformation and formation of a narrow rift at the model edge. Mechanical weakening dominates over thermal strengthening at the edge of the Class 1 models because the net heat production in the crust is low in comparison to heat flux from the mantle. Cooling due to the reduction in the thickness of the radiogenic layer in the crust during extension is thus minimal, and is countered by conduction of heat from the rising asthenosphere. In Class 1 models, the balance between cooling due to reduced radiogenic heat production (a result of thinning of the crust during extension) and warming due to the rising asthenosphere tips in favor of warming (or, at least, maintaining relatively warm temperatures) within the rift. This balance may be achieved with a range of mantle potential temperatures and crustal heat production rates, as long as the deep mantle rather than the crust dominates the thermal evolution of the uppermost mantle.

In Class 2 and 3 models, thermal strengthening dominates over mechanical weakening at the edge of the model. This is achieved by having radiogenic heat production in the crust play a more important role on determining the temperature of the uppermost mantle than in the Class 1 models. In such instances, thinning of the crust during extension results in pronounced cooling of the uppermost mantle and strengthening the lithosphere in the incipient rift zone at the eastern edge of the model. In Class 2 models, the locus of deformation is bounded on the west by strong lithosphere within the transition zone (Figs. 9–11). This causes stress to concentrate within a relatively narrow region in the interior of the WARS, between the two strong regions. Concentration of stress in this relatively narrow region leads to rapid thinning of the lithosphere. This in turn inhibits conductive cooling, allowing mechanical weakening to dominate over thermal strengthening. This leads to progressively more focused extension and formation of a narrow rift within the WARS interior, between the strong transition zone and the dynamically strengthened edge of the model. A similar process occurs in Class 3 models, but the neck develops in the transition zone between East and West Antarctica rather than in the interior of the WARS (Figs. 12–14).

The key difference between the Class 2 and Class 3 models is the initial lithosphere strength within the region of transitional lithosphere between East and West Antarctica. In Class 3 models, the transitional lithosphere is sufficiently strong to remain undeformed during the early stages of extension. The lithosphere beneath the WARS undergoes cooling and strengthening during extension, eventually becoming stronger than the unextended transitional lithosphere. When this occurs, deformation migrates into the transitional lithosphere. Focusing of extension in the narrow transitional lithosphere results in rapid thinning, minimizing thermal strengthening, and promoting progressive narrowing of the rift.

A subset of the models examined by Huerta and Harry (2007) (their class iii models) considered a much cooler lithosphere than the models shown here (T_m <680 °C). Their results show that if the lithosphere is much cooler than in the models examined here, the thermal evolution of the lithosphere has little impact on the evolution of the rift. At cooler temperatures, the horizontal temperature gradient in West Antarctica dominates model behavior from the beginning, producing a strong strength gradient that leads to rapid necking (in less than 40 m.y. after the onset of extension) at the edge of the model furthest from the cool East Antarctic craton.

Comparison to the Tectonic Evolution of West Antarctica

The Class 3 models exhibit a structural behavior that is broadly consistent with the evolution of the western half of the West Antarctic Rift System, undergoing an initial period of broad extension and then transitioning relatively abruptly to focused rifting within the transitional lithosphere between East and West Antarctica. In our best fitting model (Fig. 12), West Antarctica is initially weaker than East Antarctica (1.5×10^9 N m^{-1} versus 3.1×10^9 N m^{-1})

due to a thicker crust prior to extension (45 versus 39 km) and a higher geothermal gradient in the tectonically younger West Antarctica lithosphere (the uppermost mantle temperatures in West and East Antarctica prior to rifting are 799 °C and 665 °C, respectively). The location of the future Victoria Land Basin lies in the eastern part of the 60 km-wide transitional region between East and West Antarctica and has an intermediate crust thickness, upper mantle temperature (787 °C), and net strength (1.7×10^9 N m^{-1}). During the early stages of extension, strain is distributed throughout the relatively weak West Antarctica lithosphere (Fig. 12, 20 m.y. and 40 m.y.). The transitional region in the model, between East and West Antarctica, is initially stronger than West Antarctica and undergoes relatively little extension during this time (Figs. 12 and 13). At the relatively slow extension rate used in the models shown here, the West Antarctica lithosphere has time to cool sufficiently to eventually become stronger than the transitional region. The style of extension changes at this time, as deformation shifts into the transitional region and the broad West Antarctic Rift becomes inactive (Fig. 12, 60 m.y.). Because the transitional region is relatively narrow, stress is highly focused and the strain rate is high in this area. This results in rapid necking of the lithosphere, which inhibits cooling and strengthening and promotes formation of the narrow Terror Rift by 60 m.y. after the onset of extension. The 60 m.y. elapsed time between the onset of extension and formation of the narrow rift in the model matches the time elapsed between the Late Cretaceous onset of extension in the WARS and focusing of extension in the Terror Rift during the late Paleogene Period. The modeled width of the WARS and Victoria Land Basin, the thickness of the crust, heat flow, and elevation are in general agreement with the modern WARS (Table 3).

Implications for the Thermal State of the WARS Mantle—Plume, or No Plume?

All but two of the Class 3 models have an asthenosphere potential temperature less than 1280 °C and all have a potential temperature less than 1310 °C (Fig. 5). At higher temperatures, the models either develop a neck within the interior of the WARS (Class 2 models), or develop a neck at the edge of the model after a prolonged (ca. 100 m.y.) period of broadly distributed extension (Class 1 models). The asthenosphere potential temperature required for Class 3 model behavior is below the 1350–1400 °C suggested for mantle plumes (White and McKenzie, 1989; Sleep, 1992; Hawkesworth and Gallagher, 1993; Cagney et al., 2015), arguing against the presence of a hot mantle plume beneath the WARS during rifting in the Late Cretaceous through Paleogene Periods. The mantle potential temperature is in agreement with the relatively low temperature estimated by Perinelli et al. (2006) from pyroxene thermobarometry (1250 °C< Tp <1350 °C).

Model Limitations and Alternative Scenarios

Although the model results presented here, like those of Huerta and Harry (2007), support the argument that pre-rift and early-rift asthenosphere temperatures beneath the WARS were well below those typical of mantle plumes, there are several rifting scenarios involving mantle plumes that are not incompatible with the model results. First, the models impose a constant (adiabatic) thermal boundary condition at the base of the lithosphere. The models do not consider the effects of a late arriving (Cenozoic) plume (Hole and LeMasurier, 1994; LeMasurier and Landis, 1996; Hart et al., 1997; Sieminski et al., 2003). A late change in the temperature at the base of the lithosphere would not affect the earlier structural evolution of the rift in the models. Koptev et al. (2015) describe such a model for the East African Rift, showing that extension may focus at a cratonic edge and form a narrow rift above a rising hot plume, as in our Class 3 models. Second, the Class 3 models all require that a significant proportion of the heat that maintains the temperature of the uppermost mantle come from the crust. This is because the interior of the WARS must become cooler and stronger during rifting for the locus of extension to shift into the Victoria Land Basin region. Cooling and strengthening of the initially warm WARS lithosphere occurs in the Class 3 models because the crust, which is the heat generating layer, becomes thinner during extension. An alternative scenario, accomplishing a similar thermal evolution, would be to impose a transient heat source in the middle and lower crust. Magmatic intrusions emplaced during the long period of subduction along the WARS plate boundary may have provided such a heat source. Such intrusions may have provided sufficient heat to promote initially broad rifting, even if heat production in the crust was lower than in the models. Cooling of these fossil intrusions would promote subsequent strengthening of the lower crust, perhaps sufficiently to cause a shift in the locus of extension into the Victoria Land Basin, even in the presence of a higher asthenosphere potential temperature than imposed in the models shown here. Third, the two dimensional models examined here all impose a constant rate and direction of extension throughout the rifting episode. The timing of focusing of extension in the Victoria Land Basin is roughly coincident with the appearance of NNW-striking transtensional faults along the western WARS margin (Wilson, 1995) and with the cessation of seafloor spreading in the Adare Trough (Cande et al., 2000; Davey et al., 2006, 2016; Granot et al., 2010, 2013). These observations suggest a change in the regional stress regime during the middle Cenozoic, which may have caused a focusing of extension even if the asthenosphere was much warmer than in the Class 3

TABLE 3. COMPARISON OF BEST FIT MODEL TO WARS

Model constraint	WARS	Model
Modern WARS surface heat flux	7011–115 mW m^{-2}	72 mW m^{-2}
Modern WARS crust thickness	17–35 km	29
Modern WARS extension factor β	~2	1.9
Modern Victoria Land Basin width	180 km	~200 km
Onset of focusing in Victoria Land Basin	Late Paleocene–Late Oligocene	60 m.y.

Note: WARS—West Antarctic Rift System.

models (e.g., Salvini et al., 1997; Storti et al., 2008). Fourth, as noted by Davey et al. (2016), the Paleogene phase of rifting in the Victoria Land Basin may be unrelated to the Late Cretaceous through Late Paleogene rifting episode that included the central Ross Sea basins and may instead be associated with propagation of the seafloor spreading system in the Adare Trough southward into the Northern Basin. Although we did not explicitly model this process, we note that in such a scenario, a plume beneath the central Ross Sea would have kept the lithosphere weak in that region and would have favored propagation of Adare Trough extension into the interior of the Ross Sea rather than into the Northern Basin and Victoria Land Basin along the western margin. Finally, the low mantle potential temperatures required by the models do not preclude melting of a fossil plume (metasomatically enriched mantle), either in the asthenosphere or the lithosphere, as discussed in the Introduction.

■ SUMMARY

Finite element models show that extension of a juvenile or thermally reactivated lithosphere with warm and thick crust that is juxtaposed against older, colder cratonic lithosphere results in formation of a broad long-lived (lasting several tens of m.y.) extensional province. The formation of the broad extensional province is a robust model behavior occurring over a wide range of choices for the asthenosphere potential temperature, initial lithosphere thickness, initial crust thickness, and distribution of radiogenic heat production in the crust. Model behavior subsequent to formation of the broad extensional province depends on the interplay between shallow heat sources (the radiogenic crust) and deep heat sources (the asthenosphere). These two attributes compete to determine whether the thinning lithosphere undergoes mechanical weakening during extension as a result of concentrating extensional stress over an ever-thinning lithosphere cross section, or thermal strengthening as a result of cooling of the lithosphere. The interplay between thermal strengthening and mechanical weakening of the lithosphere during extension results in three distinct classes of model behavior, differentiated on whether and where extensional strain localizes to form a distinct rift axis after the initial period of diffuse deformation.

Class 1 models do not develop lithospheric necks during the first ca. 80 m.y. of extension. The high uppermost mantle temperatures prior to extension in these models (T_m >780 °C) minimize lateral strength variations in the lithosphere, inhibiting focusing of strain. The high asthenosphere temperatures minimize cooling during extension, keeping the lithosphere hot and weak and preventing lateral strength variations from emerging until substantial lithospheric thinning and cooling has occurred. Once that occurs, strengthening of the lithosphere within the extended and cooling WARS causes deformation to shift toward the edge of the model furthest from the cool East Antarctica craton. Focusing of extension in the relatively narrow region at the edge of the model results in accelerated thinning of the lithosphere, allowing mechanical weakening to dominate over thermal strengthening at the edge of the model.

Given sufficient extension (between 80–100 m.y. after the onset of extension in the model shown here), a distinct lithospheric neck and narrow rift ultimately form at the edge of the Class 1 models. Mechanical weakening dominates over thermal strengthening at the edge of these models because the pre-rift uppermost mantle temperature is only weakly dependent upon crustal heat generation. It results primarily from the warm and/or shallow asthenosphere rather than heat from the crust. Thinning of the heat producing layer thus has less impact on the temperature of the lithospheric mantle than does the rising hot asthenosphere. As a result, the rift axis remains warm, and deformation becomes progressively more focused.

In Class 2 models, the rift axis forms within the interior of the broad extensional province beginning ca. 40 m.y. after the onset of extension. The Class 2 models that are earliest to neck are among the warmest of the models tested, lying at the high end of the model T_p-T_m parameter space (initial T_m >890 °C and T_p >1290 °C). All Class 2 models have initial thermal properties lying in the range 1290 °C< T_p >1340 °C, T_m >820 °C, and Q_s >73 mW m^{-2}. Rift behavior in the Class 2 models is dominated by thermal strengthening at the edge of the model. In these models, crustal heat generation strongly influences the temperature at the top of the mantle. Thinning of the crust during extension results in pronounced cooling and strengthening at the edge of the model, causing deformation to shift into the now weaker interior of the broad extensional province.

Class 3 models behave similarly to Class 2 models, except the narrow rift forms within the transition zone between the formerly thicker crust of West Antarctica and the East Antarctica craton rather than within the interior of the developing WARS extensional province. The first Class 3 models to develop narrow rift axes begin to form lithospheric necks between 20 and 40 m.y. after the onset of extension, and all models of this type form distinct lithospheric necks within 80 m.y. The Class 3 models that are earliest to neck are among the coolest of the models tested, lying at the low end of the model T_p-T_m parameter space (initial T_m <780 °C and T_p <1270 °C) and opposite the parameter space position of the earliest Class 2 models. The difference in the position at which the rift axis forms in the Class 2 and Class 3 models depends on the relative strengths of the transition zone and WARS lithosphere at the end of the early (broad) phase of extension. In Class 2 models, the WARS lithosphere remains weaker than the transition zone, leading to necking within the interior of the broad extensional province. In Class 3 models, the WARS lithosphere cools sufficiently to eventually become stronger than the unextended transition zone. This causes extension to shift into the transition zone, focusing strain and forming a narrow rift.

The starting model geometry approximates that of the West Antarctic Rift System (WARS) west of Marie Byrd Land prior to the onset of extension, with a thickened West Antarctica crust simulating the thermally juvenile arc and back-arc juxtaposed against the East Antarctic craton prior to the onset of extension. The Class 3 models, in which rifting localizes within the transition zone between the craton and thicker West Antarctica crust, match in general terms the large-scale structural evolution of the WARS. In particular, the Class 3 models

match the distinctive transition from a prolonged period of broadly distributed extension beginning in the Late Cretaceous Period to a more focused style of extension within the Victoria Land Basin since Late Paleogene time. The best fitting Class 3 model (Figs. 12–14) matches the estimated duration and amount of extension in the WARS, the thickness of the crust following extension, and the timing, position, and width of extension in the Victoria Land Basin. All Class 3 models require mantle potential temperatures below 1310 °C, suggesting that a hot mantle plume was not present beneath West Antarctica during the Late Cretaceous and Paleogene Periods.

REFERENCES CITED

Accardo, N.J., Wiens, D.A., Hernandez, S., Aster, R.C., Nyblade, A., Huerta, A., Anandakrishnan, S., Wilson, T., Heeszel, D.S., and Dalziel, I.W.D., 2014, Upper mantle seismic anisotropy beneath the West Antarctic Rift System and surrounding region from shear wave splitting analysis: Geophysical Journal International, v. 198, p. 414–429, https://doi.org/10.1093/gji/ggu117.

Acton, G., Crampton, J., Di Vincenzo, G., Fielding, C.R., Florindo, F., Hannah, M., Harwood, D.M., Ishman, S., Johnson, K., Jovane, L., Levy, R., Lum, B., Marcano, M.C., Mukasa, S., Ohneiser, C., Olney, M.P., Riesselman, C., Sagnotti, L., Stefano, C., Strada, E., Taviani, M., Tuzzi, E., Verosub, K.L., Wilson, G.S., Zattin, M., and ANDRILL SMS Science Team, 2008, Preliminary Integrated Chronostratigraphy of the AND-2A Core, ANDRILL Southern McMurdo Sound Project, Antarctica: Lincoln, Nebraska, USA, University of Nebraska, ANDRILL Research and Publications Paper 6.

An, M., Wiens, D.A., Zhao, Y., Feng, M., Nyblade, A., Kanao, A., Li, Y., Maggi, A., and Leveque, J.-J., 2015, S-velocity model and inferred Moho topography beneath the Antarctic Plate from Rayleigh waves: Journal of Geophysical Research, v. 120, p. 8720–8742, https://doi.org/10.1002/2014JB011332.

Armienti, P., and Perinelli, C., 2010, Cenozoic thermal evolution of lithospheric mantle in northern Victoria Land (Antarctica): Evidences from mantle xenoliths: Tectonophysics, v. 486, p. 28–35, https://doi.org/10.1016/j.tecto.2010.02.006.

Aviado, K., Rilling-Hall, S., Bryce, J.G., and Mukasa, S.B., 2015, Submarine and subaerial lavas in the West Antarctic Rift System: Temporal record of shifting magma source components from the lithosphere and asthenosphere: Geochemistry, Geophysics, Geosystems, v. 16, p. 4344–4361, https://doi.org/10.1002/2015GC006076.

Bannister, S., Sneider, R., and Passier, M., 2000, Shear-wave velocities under the Transantarctic Mountains and Terror Rift from surface wave inversion: Geophysical Research Letters, v. 27, p. 281–284, https://doi.org/10.1029/1999GL010866.

Bannister, S., Yu, J., Leitner, B., and Kennett, B.L.N., 2003, Variations in crustal structure across the transition from West to East Antarctica, Southern Victoria Land: Geophysical Journal International, v. 155, p. 870–880, https://doi.org/10.1111/j.1365-246X.2003.02094.x.

Barrett, P.J., 2007, Cenozoic climate and sea level history from glacimarine strata off the Victoria Land coast, Capre Roberts Project, Antarctica, in Hambrey, M.J., Christoffersen, P., Glasser, N.F., and Hubbart, B., eds., Glacial Processes and Products: International Association of Sedimentologists Special Publication 39, p. 259–287.

Barrett, P.J., Elston, D.P., Harwood, D.M., Mckelvey, B.C., and Webb, P.-N., 1987, Mid-Cenozoic record of glaciation and sea-level change on the margin of the Victoria Land Basin, Antarctica: Geology, v. 15, p. 634–637, https://doi.org/10.1130/0091-7613(1987)15<634:MROGAS>2.0.CO;2.

Bartek, L.R., Henrys, S.A., Anderson, J.B., and Barrett, P.J., 1996, Seismic stratigraphy of McMurdo Sound, Antarctica: Implications for glacially influenced early Cenozoic eustatic change?: Marine Geology, v. 130, p. 79–98, https://doi.org/10.1016/0025-3227(95)00121-2.

Bassi, G., 1991, Factors controlling the style of continental rifting: Insights from numerical examples: Earth and Planetary Science Letters, v. 105, p. 430–452, https://doi.org/10.1016/0012-821X(91)90183-I.

Behrendt, J.C., and Cooper, A., 1991, Evidence of rapid Cenozoic uplift of the shoulder escarpment of the Cenozoic West Antarctic rift system and a speculation on possible climate forcing: Geology, v. 19, p. 315–319, https://doi.org/10.1130/0091-7613(1991)019<0315:EORCUO>2.3.CO;2.

Behrendt, J.C., Blankenship, D.D., Finn, C.A., Bell, R.E., Sweeney, R.E., Hodge, S.M., and Brozena, J., 1994, CASERTZ aeromagnetic data reveal Cenozoic flood basalts (?) in the West Antarctic rift system: Geology, v. 22, p. 527–530, https://doi.org/10.1130/0091-7613(1994)022<0527:CADRLC>2.3.CO;2.

Behrendt, J.C., Saltus, R., Damaske, D., McCaffrey, A., Finn, C.A., Blankenship, D., and Bell, R.E., 1996, Patterns of late Cenozoic volcanic and tectonic activity in the West Antarctic rift system revealed by aeromagnetic surveys: Tectonics, v. 15, p. 660–676, https://doi.org/10.1029/95TC03500.

Behrendt, J.C., Blankenship, D.D., Damaske, D., Cooper, A.K., Finn, C., and Bell, R.E., 1997, Geophysical evidence for late Cenozoic subglacial volcanism beneath the West Antarctic Ice Sheet and additional speculation as to its origin, in Ricci, C.A., ed., The Antarctic Region: Geological Evolution and Processes: Siena, Italy, Terra Antarctica, p. 539–546.

Berg, J.H., Moscati, R.J., and Herz, D.L., 1989, A petrologic geotherm from a continental rift in Antarctica: Earth and Planetary Science Letters, v. 93, p. 98–108, https://doi.org/10.1016/0012-821X(89)90187-8.

Bialas, R.W., Buck, W.R., Studinger, M., and Fitzgerald, P.G., 2007, Plateau collapse model for the Transantarctic Mountains-West Antarctic Rift System: Insights from numerical experiments: Geology, v. 35, no. 8, p. 687–690, https://doi.org/10.1130/G23825A.1.

Blackman, D.K., Von Herzen, R.P., and Lawver, L.A., 1987, Heat flow and tectonics in the western Ross Sea, Antarctica, in Cooper, A.K., and Davey, F.J., eds., The Antarctic Continental Margin: Geology and Geophysics of the Western Ross Sea: Houston, Texas, USA, Circum-Pacific Council for Energy and Mineral Resources, p. 179–189.

Braun, J., and Beaumont, C., 1987, Styles of continental rifting: Results from dynamic models of lithosphere extension, in Beaumont, C., and Tankard, A.J., eds., Sedimentary Basins and Basin-Forming Mechanisms: Canadian Society of Petroleum Geologists, Memoir 12, p. 241–258.

Braun, J., and Beaumont, C., 1989, Contrasting styles of lithospheric extension: Implications for differences between the Basin and Range province and rifted continental margins, in Tankard, A.J., and Balkwill, H.R., eds., Extensional Tectonics and Stratigraphy of the North Atlantic Margins: Tulsa, Oklahoma, USA, American Association of Petroleum Geologists, AAPG Memoir 46, p. 53–80.

Buck, W.R., 1991, Modes of continental lithospheric extension: Journal of Geophysical Research, v. 96, p. 20161–20178.

Buck, W.R., Lavier, L.L., and Poliakov, A.N.B., 1999, How to make a rift wide: Philosophical Transactions of the Royal Society A, v. 357, p. 671–693, https://doi.org/10.1098/rsta.1999.0348.

Bucker, C.J., Jarrard, R.D., and Wonik, T., 2001, Downhole temperature, radiogenic heat production, and heat flow from the CRP-3 drillhole, Victoria Land Basin, Antarctica: Terra Antarctica, v. 8, no. 3, p. 151–159.

Busetti, M., Spadini, G., van der Wateren, F.M., Cloetingh, S., and Zanolla, C., 1999, Kinematic modeling of the West Antarctic Rift System, Ross Sea, Antarctica: Global and Planetary Change, v. 23, p. 79–103, https://doi.org/10.1016/S0921-8181(99)00052-1.

Cagney, N., Newsome, W.H., Lithgow-Bertelloni, C., Cotel, A., Hart, S.R., and Whitehead, J.A., 2015, Temperature and velocity measurements of a rising thermal plume: Geochemistry, Geophysics, Geosystems, v. 16, no. 3, p. 579–599, https://doi.org/10.1002/2014GC005576.

Cande, S.C., Stock, J.M., Müller, R.D., and Ishihara, T., 2000, Cenozoic motion between East and West Antarctica: Nature, v. 404, p. 145–150, https://doi.org/10.1038/35004501.

Carter, N.L., and Tsenn, M.C., 1987, Flow properties of continental lithosphere: Tectonophysics, v. 136, p. 27–64, https://doi.org/10.1016/0040-1951(87)90333-7.

Chaput, J., Aster, R.C., Huerta, A., Sun, X., Lloyd, A., Wiens, D., Nyblade, A., Anandakrishnan, S., Winberry, J.P., and Wilson, T., 2014, The crustal thickness of West Antarctica: Journal of Geophysical Research, v. 119, p. 378–395, https://doi.org/10.1002/2013JB010642.

Cooper, A.F., Adam, L.J., Coulter, R.F., Eby, G.N., and McIntosh, W.C., 2007, Geology, geochronology and geochemistry of a basanitic volcano, White Island, Ross Sea, Antarctica: Journal of Volcanology and Geothermal Research, v. 165, p. 189–216, https://doi.org/10.1016/j.jvolgeores.2007.06.003.

Cooper, A.K., and Davey, F.J., 1985, Episodic rifting of Phanerozoic rocks in the Victoria Land Basin, western Ross Sea, Antarctica: Science, v. 229, p. 1085–1087, https://doi.org/10.1126/science.229.4718.1085.

Cooper, A.K., Davey, F.J., and Behrendt, J.C., 1987a, Seismic stratigraphy and structure of the Victoria Land Basin, Western Ross Sea, Antarctica, in Cooper, A.K., and Davey, F.J., eds., The Antarctic Continental Margin: Geology and Geophysics of the Western Ross Sea: Houston, Texas, USA, Circum-Pacific Council for Energy and Mineral Resources, p. 27–65.

Cooper, A.K., Davey, F.J., and Cochrane, G.R., 1987b, Structure of extensionally rifted crust beneath the western Ross Sea and Iselin Bank, Antarctica, from sonobuoy seismic data, in Cooper, A.K., and Davey, F.J., eds., The Antarctic Continental Margin; Geology and Geophysics of the Western Ross Sea, Volume 5b: Houston, Texas, USA, Circum-Pacific Council for Energy and Mineral Resources, p. 93–118.

Cooper, A.K., Davey, F.J., and Hinz, K., 1991, Crustal extension and origin of sedimentary basins beneath the Ross Sea and Ross Ice Shelf, Antarctica, in Thomson, M.R.A., Crame, J.A., and Thomson, J., eds., Geological Evolution of Antarctica: New York, USA, Cambridge University Press, p. 285–291.

Danesi, S., and Morelli, A., 2000, Group velocity of Rayleigh waves in the Antarctic region: Physics of the Earth and Planetary Interiors, v. 122, p. 55–66.

Davey, F.J., 1981, Geophysical studies in the Ross Sea: Journal of the Royal Society of New Zealand, v. 11, p. 465–479.

Davey, F.J., and Brancolini, G., 1995, The Late Mesozoic and Cenozoic structural setting of the Ross Sea region: Antarctic Research Series, v. 68, p. 167–182.

Davey, F.J., Brancolini, G., Hamilton, R.J., Henrys, S.A., Sorlien, C.C., and Bartek, L.R., 2000, A revised correlation of the seismic stratigraphy at the Cape Roberts drill sites with the seismic stratigraphy of the Victoria Land Basin, Antarctica: Terra Antartica, v. 7, no. 3, p. 215–220.

Davey, F.J., Cande, S.C., and Stock, J.M., 2006, Extension in the western Ross Sea region-links between Adare Basin and Victoria Land Basin: Geophysical Research Letters, v. 33, https://doi.org/10.1029/2006GL027383.

Davey, F.J., Granot, R., Cande, S.C., Stock, J.M., Selvans, M., and Ferraccioli, F., 2016, Synchronous oceanic spreading and continental rifting in West Antarctica: Geophysical Research Letters, v. 43, p. 6162–6169, https://doi.org/10.1002/2016GL069087.

Decesari, R.C., Sorlien, C.C., Luyendyk, B.P., Wilson, D.S., and Bartek, L.R., 2008a, Regional seismic stratigraphic correlations of the Ross Sea: Implications for the tectonic history of the West Antarctic Rift System, in Cooper, A.K., Barrett, P.J., Stagg, H., Storey, B., Stump, E., Wise, W., Anderson, J., Barron, J., Bart, P., Blankenship, D., Davey, F., Diggles, M., Finn, C., Fitzgerald, P., Florindo, F., Francis, J., Futterer, D., Gamble, J., Goodge, J., Hammer, W., Helton, P., Ivins, E., Kyle, P., LeMasurier, W., Mayewski, P., Naish, T., Passchier, S., Pekar, S., Raymond, C., Ricci, C.A., Studinger, M., Sugden, D., Thorn, V., and Wilson, T., eds., Antarctica: A Keystone in a Changing World: Washington, D.C., USA, The National Academies Press Proceedings of the 10th International Symposium on Antarctic Earth Sciences, https://doi.org/10.3133/of2007-1047.srp052.

Decesari, R.C., Wilson, D.S., Luyendyk, B.P., and Faulkner, M., 2008b, Cretaceous and Tertiary extension throughout the Ross Sea, Antarctica, in Cooper, A.K., Barrett, P.J., Stagg, H., Storey, B., Stump, E., Wise, W., Anderson, J., Barron, J., Bart, P., Blankenship, D., Davey, F., Diggles, M., Finn, C., Fitzgerald, P., Florindo, F., Francis, J., Futterer, D., Gamble, J., Goodge, J., Hammer, W., Helton, P., Ivins, E., Kyle, P., LeMasurier, W., Mayewski, P., Naish, T., Passchier, S., Pekar, S., Raymond, C., Ricci, C.A., Studinger, M., Sugden, D., Thorn, V., and Wilson, T., eds., Antarctica: A Keystone in a Changing World: Washington, D.C., USA, The National Academies Press Proceedings of the 10th International Symposium on Antarctic Earth Sciences.

Dunbar, J.A., and Sawyer, D.S., 1989, How preexisting weaknesses control the style of continental breakup: Journal of Geophysical Research, v. 94, p. 7278–7292, https://doi.org/10.1029/JB094iB06p07278.

Eagles, G., 2003, Tectonic evolution of the Antarctic-Phoenix plate system since 15 Ma: Earth and Planetary Science Letters, v. 217, no. 102, p. 97–109.

Eagles, G., Gohl, K., and Larter, R.D., 2004, High-resolution animated tectonic reconstruction of the South Pacific and West Antarctic Margin: Geochemistry, Geophysics, Geosystems, v. 5, no. 7, https://doi.org/10.1029/2003GC000657.

Eagles, G., Gohl, K., and Larter, R.D., 2009, Animated tectonic reconstruction of the Southern Pacific and alkaline volcanism at its convergent margins since Eocene times: Tectonophysics, v. 464, p. 21–29, https://doi.org/10.1016/j.tecto.2007.10.005.

Elliot, D.H., 1992, Jurassic magmatism and tectonism associated with Gondwanaland break-up: An Antarctic perspective, in Storey, B.C., Alabaster, T., and Pankhurst, R.J., eds., Magmatism and the Causes of Continental Break-up: Geological Society of London Special Publication 68, p. 165–184, https://doi.org/10.1144/GSL.SP.1992.068.01.11.

Emry, E.L., Nyblade, A.A., Julià, J., Anandakrishnan, S., Aster, R.C., Wiens, D.A., Huerta, A.D., and Wilson, T.J., 2015, The mantle transition zone beneath West Antarctica: Seismic evidence for hydration and thermal upwellings: Geochemistry, Geophysics, Geosystems, v. 16, no. 1, p. 40–58, https://doi.org/10.1002/2014GC005588.

Esser, R.P., Kyle, P.R., and McIntosh, W.C., 2004, $^{40}Ar/^{39}Ar$ dating of the eruptive history of Mount Erebus, Antarctica: Volcano evolution: Bulletin of Volcanology, v. 66, p. 671–686, https://doi.org/10.1007/s00445-004-0354-x.

Ferraccioli, F., Coren, F., Bozzo, E., Zanolla, C., Gandolfi, S., Tabacco, I., and Frezzotti, M., 2001, Rifted(?) crust at the East Antarctic Craton margin: Gravity and magnetic interpretation along a traverse across the Wilkes Subglacial Basin region: Earth and Planetary Science Letters, v. 192, p. 407–421, https://doi.org/10.1016/S0012-821X(01)00459-9.

Ferraccioli, F., Armadillo, E., Zunino, A., Bozzo, E., Rocchi, S., and Armienti, P., 2009, Magmatic and tectonic patterns over the Northern Victoria Land sector of the Transantarctic Mountains from new aeromagnetic imaging: Tectonophysics, v. 478, p. 43–61, https://doi.org/10.1016/j.tecto.2008.11.028.

Ferraccioli, F., Finn, C.A., Jordan, T.A., Bell, R.E., Anderson, L.M., and Damaske, D., 2011, East Antarctic rifting triggers uplift of the Gamburtsev Mountains: Nature, v. 479, p. 388–392, https://doi.org/10.1038/nature10566.

Fielding, C.R., Whittaker, J., Henrys, S.A., Wilson, T.J., and Naish, T.R., 2008a, Seismic facies and stratigraphy of the Cenozoic succession in McMurdo Sound, Antarctica: Implications for tectonic, climatic and glacial history, in Cooper, A.K., Barrett, P.J., Stagg, H., Storey, B., Stump, E., Wise, W., Anderson, J., Barron, J., Bart, P., Blankenship, D., Davey, F., Diggles, M., Finn, C., Fitzgerald, P., Florindo, F., Francis, J., Futterer, D., Gamble, J., Goodge, J., Hammer, W., Helton, P., Ivins, E., Kyle, P., LeMasurier, W., Mayewski, P., Naish, T., Passchier, S., Pekar, S., Raymond, C., Ricci, C.A., Studinger, M., Sugden, D., Thorn, V., and Wilson, T., eds., Antarctica: A Keystone in a Changing World: Washington, D.C., USA, The National Academies Press Proceedings of the 10th International Symposium on Antarctic Earth Sciences, https://doi.org/10.3133/of2007-1047.srp09.

Fielding, C.R., Whittaker, J., Henrys, S.A., Wilson, T.J., and Naish, T.R., 2008b, Seismic facies and stratigraphy of the Cenozoic succession in McMurdo Sound, Antarctica: Implications for tectonic, climatic and glacial history: Palaeogeography, Palaeoclimatology, Palaeoecology, v. 260, p. 8–29, https://doi.org/10.1016/j.palaeo.2007.08.016.

Finn, C.A., Müller, R.D., and Panter, K.S., 2005, A Cenozoic diffuse alkaline magmatic province (DAMP) in the southwest Pacific without rift or plume origin: Geochemistry, Geophysics, Geosystems, v. 6, https://doi.org/10.1029/2004GC000723.

Finotello, M., Nyblade, A., Julia, J., Wiens, D., and Anandakrishnan, S., 2011, Crustal Vp-Vs ratios and thickness of Ross Island and the Transantarctic Mountain front, Antarctica: Geophysical Journal International, v. 185, p. 85–92, https://doi.org/10.1111/j.1365-246X.2011.04946.x.

Fitzgerald, P.G., 2002, Tectonics and landscape evolution of the Antarctic plate since the breakup of Gondwana, with an emphasis on the West Antarctic Rift System and the Transantarctic Mountains: Royal Society of New Zealand Bulletin, v. 35, p. 453–469.

Fitzgerald, P.G., Bialas, R.W., Buck, W.R., and Studinger, M., 2008, A plateau collapse model for the formation of the West Antarctic rift system/Transantarctic Mountains, in Cooper, A.K., Barrett, P.J., Stagg, H., Storey, B., Stump, E., Wise, W., Anderson, J., Barron, J., Bart, P., Blankenship, D., Davey, F., Diggles, M., Finn, C., Fitzgerald, P., Florindo, F., Francis, J., Futterer, D., Gamble, J., Goodge, J., Hammer, W., Helton, P., Ivins, E., Kyle, P., LeMasurier, W., Mayewski, P., Naish, T., Passchier, S., Pekar, S., Raymond, C., Ricci, C.A., Studinger, M., Sugden, D., Thorn, V., and Wilson, T., eds., Antarctica: A Keystone in a Changing World: Washington, D.C., USA, The National Academies Press Proceedings of the 10th International Symposium on Antarctic Earth Sciences, Extended Abstract 087.

Futa, K., and LeMasurier, W.E., 1983, Nd and Sr isotopic studies on Cenozoic mafic lavas from West Antarctica: Another source for continental alkali basalts: Contributions to Mineralogy and Petrology, v. 83, p. 38–44, https://doi.org/10.1007/BF00373077.

Granot, R., Cande, S.C., Stock, J.M., Davey, F.J., and Clayton, R.W., 2010, Postspreading rifting in the Adare Basin, Antarctica: Regional tectonic consequences: Geochemistry, Geophysics, Geosystems, v. 11, no. 8, https://doi.org/10.1029/2010GC003105.

Granot, R., Cande, S.C., Stock, J.M., and Damaske, D., 2013, Revised Eocene-Oligocene kinematics for the West Antarctic rift system: Geophysical Research Letters, v. 40, p. 279–284, https://doi.org/10.1029/2012GL054181.

Graw, J.H., Adams, A.N., Hansen, S.E., Wiens, D.A., Hackworth, L., and Park, Y., 2016, Upper mantle shear wave velocity structure beneath northern Victoria Land, Antarctica: Volcanism and uplift in the northern Transantarctic Mountains: Earth and Planetary Science Letters, v. 449, p. 48–60, https://doi.org/10.1016/j.epsl.2016.05.026.

Gupta, S., Zhao, D., and Rai, S., 2009, Seismic imaging of the upper mantle under Erebus hotspot in Antarctica: Gondwana Research, v. 16, p. 109–118, https://doi.org/10.1016/j.gr.2009.01.004.

Hall, J., Wilson, T., and Henrys, S., 2008, Structure of the central Terror Rift, western Ross Sea, Antarctica, *in* Cooper, A.K., Barrett, P.J., Stagg, H., Storey, B., Stump, E., Wise, W., Anderson, J., Barron, J., Bart, P., Blankenship, D., Davey, F., Diggles, M., Finn, C., Fitzgerald, P., Florindo, F., Francis, J., Futterer, D., Gamble, J., Goodge, J., Hammer, W., Helton, P., Ivins, E., Kyle, P., LeMasurier, W., Mayewski, P., Naish, T., Passchier, S., Pekar, S., Raymond, C., Ricci, C.A., Studinger, M., Sugden, D., Thorn, V., and Wilson, T., eds., Antarctica: A Keystone in a Changing World: Washington, D.C., USA, The National Academies Press Proceedings of the 10th International Symposium on Antarctic Earth Sciences.

Hamilton, R.J., Luyendyk, B.P., Sorlien, C.C., and Bartek, L.R., 2001, Cenozoic tectonics of the Cape Roberts rift basin and Transantarctic Mountains front, southwestern Ross Sea, Antarctica: Tectonics, v. 20, p. 325–342, https://doi.org/10.1029/2000TC001218.

Hansen, S.E., Julia, J., Nyblade, A., Pyle, M.L., Wiens, D.A., and Anandakrishnan, A., 2009, Using S wave receiver functions to estimate crustal structure beneath ice sheets: An application to the Transantarctic Mountains and East Antarctic craton: Geochemistry, Geophysics, Geosystems, v. 10, https://doi.org/10.1029/2009GC002576.

Hansen, S.E., Nyblade, A., Heeszel, D.S., Wiens, D.A., Shore, P.J., and Kanao, M., 2010, Crustal structure of the Gamburtsev Mountains, East Antarctica, from S-wave receiver functions and Rayleigh wave phase velocities: Earth and Planetary Science Letters, v. 300, p. 395–401, https://doi.org/10.1016/j.epsl.2010.10.022.

Hansen, S.E., Graw, J.H., Kenyon, L.M., Nyblade, A.A., Wiens, D.A., Aster, R.C., Huerta, A.D., and Anadakrishnan, S., 2014, Imaging the Antarctic mantle using adaptively parameterized P-wave tomography: Evidence for heterogeneous structure beneath West Antarctica: Earth and Planetary Science Letters, v. 408, p. 66–78, https://doi.org/10.1016/j.epsl.2014.09.043.

Hansen, S.E., Kenyon, L.M., Graw, J.H., Park, Y., and Nyblade, A., 2016, Crustal structure beneath the Northern Transantarctic Mountains and Wilkes Subglacial Basin: Implications for tectonic origins: Journal of Geophysical Research, v. 121, p. 812–825, https://doi.org/10.1002/2015JB012325.

Harry, D.L., Sawyer, D.S., and Leeman, W.P., 1993, The mechanics of continental extension in western North America: Implications for the magmatic and structural evolution of the Great Basin: Earth and Planetary Science Letters, v. 117, p. 59–71, https://doi.org/10.1016/0012-821X(93)90117-R.

Hart, S.R., Blusztajn, J., LeMasurier, W.E., and Rex, D.C., 1997, Hobbs Coast Cenozoic volcanism: Implications for the West Antarctic rift system: Chemical Geology, v. 139, p. 223–248, https://doi.org/10.1016/S0009-2541(97)00037-5.

Hawkesworth, C.J., and Gallagher, K., 1993, Mantle hotspots, plumes and regional tectonics as causes of intraplate magmatism: Terra Nova, v. 5, p. 552–559, https://doi.org/10.1111/j.1365-3121.1993.tb00304.x.

Heeszel, D.S., Wiens, D.A., Anandakrishnan, S., Aster, R.C., Dalziel, I.W.D., Huerta, A., Nyblade, A., Wilson, T.J., and Winberry, J.P., 2016, Upper mantle structure of central and West Antarctica from array analysis of Rayleigh wave phase velocities: Journal of Geophysical Research, v. 121, no. 3, p. 1758–1775, https://doi.org/10.1002/2015JB012616.

Henrys, S.A., Wilson, T.J., Fielding, C.R., Hall, J., and Naish, T.R., 2008, Tectonic history of mid-Miocene to present southern Victoria Land Basin, inferred from seismic stratigraphy in McMurdo Sound, Antarctica, *in* Cooper, A.K., Barrett, P.J., Stagg, H., Storey, B., Stump, E., Wise, W., Anderson, J., Barron, J., Bart, P., Blankenship, D., Davey, F., Diggles, M., Finn, C., Fitzgerald, P., Florindo, F., Francis, J., Futterer, D., Gamble, J., Goodge, J., Hammer, W., Helton, P., Ivins, E., Kyle, P., LeMasurier, W., Mayewski, P., Naish, T., Passchier, S., Pekar, S., Raymond, C., Ricci, C.A., Studinger, M., Sugden, D., Thorn, V., and Wilson, T., eds., Antarctica: A Keystone in a Changing World: Washington, D.C., USA, The National Academies Press Proceedings of the 10th International Symposium on Antarctic Earth Sciences, https://doi.org/10.3133/of2007-1047.srp049.

Hole, M.J., and LeMasurier, W.E., 1994, Tectonic controls on the geochemical composition of Cenozoic, mafic alkaline volcanic rocks from West Antarctica: Contributions to Mineralogy and Petrology, v. 117, p. 187–202, https://doi.org/10.1007/BF00286842.

Hopper, J.R., and Buck, W.R., 1993, The initiation of rifting at constant tectonic force: Role of diffusion creep: Journal of Geophysical Research, v. 98, p. 16,213–16,221, https://doi.org/10.1029/93JB01725.

Hopper, J.R., and Buck, W.R., 1996, The effect of lower crustal flow on continental extension and passive margin formation: Journal of Geophysical Research, v. 101, p. 20175–20194.

Huerta, A.D., 2008, Byrd drainage system: Evidence of a Mesozoic West Antarctic Plateau, *in* Cooper, A.K., Barrett, P.J., Stagg, H., Storey, B., Stump, E., Wise, W., Anderson, J., Barron, J., Bart, P., Blankenship, D., Davey, F., Diggles, M., Finn, C., Fitzgerald, P., Florindo, F., Francis, J., Futterer, D., Gamble, J., Goodge, J., Hammer, W., Helton, P., Ivins, E., Kyle, P., LeMasurier, W., Mayewski, P., Naish, T., Passchier, S., Pekar, S., Raymond, C., Ricci, C.A., Studinger, M., Sugden, D., Thorn, V., and Wilson, T., eds., Antarctica: A Keystone in a Changing World: Washington, D.C., USA, The National Academies Press Proceedings of the 10th International Symposium on Antarctic Earth Sciences, Extended Abstract 092.

Huerta, A.D., and Harry, D.L., 2007, The transition from diffuse to focused extension: Modeled evolution of the West Antarctic Rift system: Earth and Planetary Science Letters, v. 255, p. 133–147, https://doi.org/10.1016/j.epsl.2006.12.011.

Jones, S., 1996, Late Quaternary faulting and neotectonics, South Victoria Land, Antarctica: Journal of the Geological Society, v. 153, p. 645–652.

Jordan, T.A., Ferraccioli, F., Ross, N., Coore, H.J., Leat, P.T., Bingham, R.G., Rippin, D.M., le Brocq, A., and Siegert, M.J., 2013, Inland extent of the Weddell Sea Rift imaged by new aerogeophysical data: Tectonophysics, v. 585, p. 137–160, https://doi.org/10.1016/j.tecto.2012.09.010.

Jordan, T.A., Ferraccioli, F., and Leat, P.T., 2017, New geophysical compilations link crustal block motion to Jurassic extension and strike-slip faulting in the Weddell Sea Rift System of West Antarctica: Gondwana Research, v. 42, p. 29–48, https://doi.org/10.1016/j.gr.2016.09.009.

Koptev, A., Dalais, E., Burov, E., Leroy, S., and Gerya, T., 2015, Dual continental rift systems generated by plume–lithosphere interaction: Nature Geoscience, v. 8, p. 388–392, https://doi.org/10.1038/ngeo2401.

Kula, J., Tulloch, A., Spell, T.L., and Wells, M.L., 2007, Two-stage rifting of Zealandia-Australia-Antarctica: Evidence from $^{40}Ar/^{39}Ar$ thermochronometry of the Sisters shear zone, Stewart Island, New Zealand: Geology, v. 35, no. 5, p. 411–414, https://doi.org/10.1130/G23432A.1.

Kyle, R., 1990, McMurdo Volcanic Group, western Ross Embayment: Introduction, *in* LeMasurier, W.E., and Thompson, J.W., eds., Volcanoes of the Antarctic Plate and Southern Ocean, Antarctic Research Series, Volume 48: Washington, D.C., USA, American Geophysical Union, p. 19–25, https://doi.org/10.1029/90EO00230.

Larter, R.D., Cunningham, A., Barker, P.F., Gohl, K., and Nitsche, F.O., 2002, Tectonic evolution of the Pacific margin of Antarctica 1. Late Cretaceous tectonic reconstructions: Journal of Geophysical Research, v. 107, no. B12, https://doi.org/10.1029/2000JB000052.

Lawrence, J.F., Wiens, D.A., Nyblade, A.A., Anandakrishnan, S., Shore, P.J., and Voigt, D., 2006a, Rayleigh wave phase velocity analysis of the Ross Sea, Transantarctic Mountains, and East Antarctica from a temporary seismograph array: Journal of Geophysical Research, B06302, https://doi.org/10.1029/2005JB003812.

Lawrence, J.F., Wiens, D.A., Nyblade, A.A., Anandakrishnan, S., Shore, P.J., and Voigt, D., 2006b, Crust and upper mantle structure of the Transantarctic Mountains and surrounding regions from receiver functions, surface waves, and gravity: Implications for uplift models: Geochemistry, Geophysics, Geosystems, v. 7, https://doi.org/10.1029/2006GC001282.

Lawver, L.A., and Gahagan, L.M., 1994, Constraints on timing of extension in the Ross Sea region: Terra Antarctica, v. 1, no. 3, p. 545–552.

Lawver, L.A., Gahagan, L.M., and Coffin, M.F., 1992, The development of paleoseaways around Antarctica, *in* Kennett, J.P., and Warkne, D.A., eds., The Antarctic Paleoenvironment: Perspectives on Global Change: Part One: Washington, D.C., USA, American Geophysical Union, Antarctic Research Series, v. 56, p. 7–30.

LeMasurier, W.E., 2006, What supports the Marie Byrd Land Dome? An Evaluation of Potential Uplift Mechanisms in a Continental Rift System, *in* Futterer, D.K., Damaske, D., Kleinschmidt, G., Miller, H., Tessensoh, F., eds., Antarctica: Contributions to Global Earth Sciences: Berlin, Germany, Springer-Verlag, p. 299–302, https://doi.org/10.1007/3-540-32934-X_37.

LeMasurier, W.E., 2008, Neogene extension and basin deepening in the West Antarctic rift inferred from comparisons with the East African rift and other analogs: Geology, v. 36, no. 3, p. 247–250, https://doi.org/10.1130/G24363A.1.

LeMasurier, W.E., and Landis, C.A., 1996, Mantle-plume activity recorded by low-relief erosion surfaces in West Antarctica and New Zealand: Geological Society of America Bulletin, v. 108, p. 1450–1466, https://doi.org/10.1130/0016-7606(1996)108<1450:MPARBL>2.3.CO;2.

LeMasurier, W.E., and Rex, D.C., 1991, The Marie Byrd Land volcanic province and its relation to the Cainozoic West Antarctic rift system, *in* Tingey, R.J., ed., The Geology of Antarctica: New York, USA, Clarendon Press, p. 249–284.

Lisker, F., and Laufer, A.L., 2013, The Mesozoic Victoria Basin: Vanished link between Antarctica and Australia: Geology, v. 41, p. 1043–1046, https://doi.org/10.1130/G33409.1.

Lloyd, A.J., Weins, D.A., Nyblade, A.A., Anandakrishnan, A., Aster, R.C., Huerta, A.D., Wilson, T.J., Dalziel, I.W.D., Shore, P.J., and Zhao, D., 2015, A seismic transect across West Antarctica: Evidence for mantle thermal anomalies beneath the Bentley Subglacial Trench and the Marie Byrd Land Dome: Journal of Geophysical Research, v. 120, p. 8439–8460, https://doi.org/10.1002/2015JB012455.

Llubes, M., Florsch, N., Legresy, B., Lemoine, J.-M., Loyer, S., Crossley, D., and Remy, F., 2003, Crustal thickness in Antarctica from CHAMP gravimetry: Earth and Planetary Science Letters, v. 212, p. 103–117, https://doi.org/10.1016/S0012-821X(03)00245-0.

Luyendyk, B.P., 1995, Hypothesis for Cretaceous rifting of east Gondwana caused by subducted slab capture: Geology, v. 23, p. 373–376, https://doi.org/10.1130/0091-7613(1995)023<0373:HFCROE>2.3.CO;2.

Luyendyk, B.P., Cisowksi, S., Smith, C.H., Richard, S.M., and Kimbrough, D.L., 1996, Paleomagnetic study of the northern Ford Ranges, western Marie Byrd Land, West Antarctica: A middle Cretaceous pole, and motion between West and East Antarctica?: Tectonics, v. 15, p. 122–141, https://doi.org/10.1029/95TC02524.

Luyendyk, B.P., Sorlien, C.C., Wilson, D.S., Bartek, L.R., and Siddoway, C.S., 2001, Structural and tectonic evolution of the Ross Sea Rift in the Cape Colbeck region, eastern Ross Sea, Antarctica: Tectonics, v. 20, no. 6, p. 933–958, https://doi.org/10.1029/2000TC001260.

Luyendyk, B.P., Wilson, D.S., and Siddoway, C.S., 2003, Eastern margin of the Ross Sea Rift in western Marie Byrd Land, Antarctica: Crustal structure and tectonic development: Geochemistry, Geophysics, Geosystems, v. 4, no. 10, https://doi.org/10.1029/2002GC000462.

McGinnis, L.D., Bowen, R.H., Erickson, J.M., Allred, B.J., and Kreamer, J.L., 1985, East-West Antarctic boundary in McMurdo Sound, in Husebye Eystein, S., Johnson, G.L., and Kristoffersen, Y., eds., Geophysics of the Polar Regions: Amsterdam, Netherlands, Elsevier, v. 114, no. 1–4, p. 341–356.

Morelli, A., and Danesi, S., 2004, Seismological imaging of the Antarctic lithosphere: A review: Global and Planetary Change, v. 42, p. 155–165, https://doi.org/10.1016/j.gloplacha.2003.12.005.

Morin, R.H., Williams, T., Henrys, S.A., Magens, D., Niessen, F., and Hansaraj, D., 2010, Heat flow and hydrologic characteristics at the AND-1B borehole, ANDRILL McMurdo Ice Shelf Project, Antarctica: Geosphere, v. 6, no. 4, p. 370–378, https://doi.org/10.1130/GES00512.1.

Mukasa, S.B., and Dalziel, I.W.D., 2000, Marie Byrd Land, West Antarctica: Evolution of Gondwana's Pacific margin constrained by zircon U-Pb geochronology and feldspar common-Pb isotopic compositions: Geological Society of America Bulletin, v. 112, no. 4, p. 611–627, https://doi.org/10.1130/0016-7606(2000)112<611:MBLWAE>2.0.CO;2.

Müller, R.D., Cande, S.C., Stock, J.M., and Keller, W.R., 2005, Crustal structure and rift flank uplift of the Adare Trough, Antarctica: Geochemistry, Geophysics, Geosystems, v. 6, no. 11, https://doi.org/10.1029/2005GC001027.

Müller, R.D., Gohl, K., Cande, S.C., Goncharov, A., and Golynsky, A.V., 2007, Eocene to Miocene geometry of the West Antarctic Rift System: Australian Journal of Earth Sciences, v. 54, p. 1033–1045, https://doi.org/10.1080/08120090701615691.

Naish, T., Powel, R., Levy, R., Henrys, S., Krissek, L., Niessen, F., Pompilio, M., Scherer, R., and Wilson, G., 2007, Synthesis of the Initial Scientific Results of the MIS Project (AND-1B Core), Victoria Land Basin, Antarctica: Terra Antartica, v. 14, no. 3, p. 317–327.

Nardini, I., Armienti, P., Rocchi, S., Dallai, L., and Harrison, D., 2009, Sr-Nd-Pb-He-O isotope and geochemical constraints on the genesis of Cenozoic magmas from the West Antarctic Rift: Journal of Petrology, v. 50, p. 1359–1375, https://doi.org/10.1093/petrology/egn082.

National Geodetic Data Center, 2006, 2-minute Gridded Global Relief Data (ETOPO2) v2, National Geophysical Data Center, National Oceanic and Atmospheric Administration, https://doi.org/10.7289/V5J1012Q.

O'Donnell, J.P., and Nyblade, A., 2014, Antarctica's hypsometry and crustal thickness: Implications for the origin of anomalous topography in East Antarctica: Earth and Planetary Science Letters, v. 388, p. 143–155, https://doi.org/10.1016/j.epsl.2013.11.051.

O'Donnell, J.P., Selway, K., Nyblade, A.A., Brazier, R.A., Wiens, D.A., Anandakrishnan, S., Aster, R.C., Huerta, A., Wilson, T., and Winberry, J.P., 2017, The uppermost mantle seismic velocity and viscosity structure of central West Antarctica: Earth and Planetary Science Letters, v. 472, p. 38–49, https://doi.org/10.1016/j.epsl.2017.05.016.

Panter, K.S., Hart, S.R., Kyle, P.R., Blusztanjn, J., and Wilch, T., 2000, Geochemistry of Late Cenozoic basalts from the Crary Mountains: Characterization of mantle sources in Marie Byrd Land, Antarctica: Chemical Geology, v. 165, p. 215–241, https://doi.org/10.1016/S0009-2541(99)00171-0.

Panter, K.S., Blusztanjn, J., Hart, S.R., Kyle, P.R., Esser, R.P., and McIntosh, W.C., 2006, The origin of HIMU in the SW Pacific: Evidence from intraplate volcanism in southern New Zealand and subantarctic islands: Journal of Petrology, v. 47, p. 1673–1704, https://doi.org/10.1093/petrology/egl024.

Paulsen, T., Wilson, T.J., Demosthenous, C., Millan, C., Jarrard, R., and Laufer, A.L., 2014, Kinematics of the Neogene Terror Rift: Constraints from calcite twinning strains in the ANDRILL McMurdo Ice Shelf (AND-1B) core, Victoria Land Basin, Antarctica: Geosphere, v. 10, p. 828–841, https://doi.org/10.1130/GES01002.1.

Paulsen, T.S., and Wilson, T.J., 2009, Structure and age of volcanic fissures on Mount Morning: A new constraint on Neogene contemporary stress in the West Antarctic Rift, southern Victoria Land, Antarctica: Geological Society of America Bulletin, v. 121, p. 1071–1088, https://doi.org/10.1130/B26333.1.

Perinelli, C., Armienti, P., and Dallai, L., 2006, Geochemical and O-isotope constraints on the evolution of lithospheric mantle in the Ross Sea rift area (Antarctica): Contributions to Mineralogy and Petrology, v. 151, p. 245–266, https://doi.org/10.1007/s00410-006-0065-8.

Powell, R.D., Laird, M.G., Naish, T.R., Fielding, C.R., Krissek, L.A., and van der Meer, J.J.M., 2001, Depositional environments for strata cored in CRP-3 (Cape Roberts Project), Victoria Land Basin, Antarctica: Palaeoglaciological and palaeoclimatological inferences: Terra Antartica, v. 8, p. 207–216.

Pyle, M.L., Wiens, D.A., Nyblade, A.A., and Anandakrishnan, S., 2010, Crustal structure of the Transantarctic Mountains near the Ross Sea from ambient seismic noise tomography: Journal of Geophysical Research, v. 115, B11310, https://doi.org/10.1029/2009JB007081.

Ranalli, G., and Murphy, D.C., 1987, Rheological stratification of the lithosphere: Tectonophysics, v. 132, p. 281–295, https://doi.org/10.1016/0040-1951(87)90348-9.

Rilling, R.E., Mukasa, S.B., Wilson, T.J., and Lawver, L.A., 2008, 40Ar-39Ar Age constraints on volcanism and tectonism in the Terror Rift of the Ross Sea, Antarctica, in Cooper, A.K., Barrett, P.J., Stagg, H., Storey, B., Stump, E., Wise, W., Anderson, J., Barron, J., Bart, P., Blankenship, D., Davey, F., Diggles, M., Finn, C., Fitzgerald, P., Florindo, F., Francis, J., Futterer, D., Gamble, J., Goodge, J., Hammer, W., Helton, P., Ivins, E., Kyle, P., LeMasurier, W., Mayewski, P., Naish, T., Passchier, S., Pekar, S., Raymond, C., Ricci, C. A., Studinger, M., Sugden, D., Thorn, V., and Wilson, T., eds., Antarctica: A Keystone in a Changing World: Washington, D.C., USA, The National Academies Press Proceedings of the 10th International Symposium on Antarctic Earth Sciences.

Ritzwoller, M.H., Shapiro, N.M., Levshin, A.L., and Leahy, G.M., 2001, Crustal and upper mantle structure beneath Antarctica and surrounding oceans: Journal of Geophysical Research, v. 106, p. 30645–30670, https://doi.org/10.1029/2001JB000179.

Roberts, A.P., Wilson, G.S., Harwood, D.M., and Verosub, K.L., 2003, Glaciation across the Oligocene-Miocene boundary in southern McMurdo Sound, Antarctica: New chronology from the CIROS-1 drill hole: Palaeogeography, Palaeoclimatology, Palaeoecology, v. 198, p. 113–130, https://doi.org/10.1016/S0031-0182(03)00399-7.

Rocchi, S., Armienti, P., D'Orazio, M., Tonarini, S., Wijbrans, J.R., and Vincenzo, G.D., 2002, Cenozoic magmatism in the western Ross Embayment: Role of mantle plume versus plate dynamics in the development of the West Antarctic Rift System: Journal of Geophysical Research, v. 107, B9, https://doi.org/10.1029/2001JB000515.

Rocchi, S., Armienti, P., and Vincenzo, G.D., 2005, No plume, no rift magmatism in the West Antarctic Rift, in Folger, G.R., Natland, J.H., Presnall, D.C., and Anderson, D.L., eds., Plates, Plumes, and Paradigms: Geological Society of America Special Paper 388, p. 435–447, https://doi.org/10.1130/0-8137-2388-4.435.

Rocholl, A., Stein, M., Molzahn, M., Hart, S.R., and Wörner, G., 1995, Geochemical evolution of rift magmas by progressive tapping of a stratified mantle source beneath the Ross Sea Rift, Northern Victoria Land, Antarctica: Earth and Planetary Science Letters, v. 131, p. 207–224, https://doi.org/10.1016/0012-821X(95)00024-7.

Rossetti, F., Storti, F., Busetti, M., Lisker, F., Vicenzo, G.D., Laufer, A.L., Rocchi, S., and Salvini, F., 2006, Eocene initiation of Ross Sea dextral faulting and implications for East Antarctic neotectonics: Journal of the Geological Society, v. 163, p. 119–126, https://doi.org/10.1144/0016-764905-005.

Roult, G., Rouland, D., and Montagner, J.P., 1994, Antarctica II: Upper-mantle structure from velocities and anisotropy: Physics of the Earth and Planetary Interiors, v. 84, p. 33–57, https://doi.org/10.1016/0031-9201(94)90033-7.

Salvini, F., Brancolini, G., Busetti, M., Storti, F., Mazzarini, F., and Coren, F., 1997, Cenozoic geodynamics of the Ross Sea region, Antarctic: Crustal extension, intraplate strike-slip faulting, and tectonic inheritance: Journal of Geophysical Research, v. 102, p. 24669–24696.

Schroder, H., Paulsen, T., and Wonik, T., 2011, Thermal properties of the AND-2A borehole in the southern Victoria Land Basin, McMurdo Sound, Antarctica: Geosphere, v. 7, no. 6, p. 1324–1330, https://doi.org/10.1130/GES00690.1.

Schwartz, J.J., Stowell, H.H., Klepies, K., Tulloch, A.J., Kylander-Clark, R.C., Hacker, B.R., and Coble, M.A., 2016, Thermochronology of extensional orogenic collapse in the deep crust of Zealandia: Geosphere, v. 12, no. 3, p. 647–677, https://doi.org/10.1130/GES01232.1.

Scott, J.M., Waight, T.E., van der Meer, Q.H.A., Palin, J.M., Cooper, A.F., and Münker, C., 2014, Metasomatized ancient lithospheric mantle beneath the young Zealandia microcontinent and its role in HIMU-like intraplate magmatism: Geochemistry, Geophysics, Geosystems, v. 15, p. 3477–3501, https://doi.org/10.1002/2014GC005300.

Siddoway, C.S., 2008, Tectonics of the West Antarctic Rift System: New light on the history and dynamics of distributed intracontinental extension, in Cooper, A.K., Barrett, P.J., Stagg, H., Storey, B., Stump, E., Wise, W., Anderson, J., Barron, J., Bart, P., Blankenship, D., Davey, F., Diggles, M., Finn, C., Fitzgerald, P., Florindo, F., Francis, J., Futterer, D., Gamble, J., Goodge, J., Hammer, W., Helton, P., Ivins, E., Kyle, P., LeMasurier, W., Mayewski, P., Naish, T., Passchier, S., Pekar, S., Raymond, C., Ricci, C.A., Studinger, M., Sugden, D., Thorn, V., and Wilson, T., eds., Antarctica: A Keystone in a Changing World: Washington, D.C., USA, The National Academies Press Proceedings of the 10th International Symposium on Antarctic Earth, p. 91–114.

Siddoway, C.S., Baldwin, S.L., Fitzgerald, P.G., Fanning, C.M., and Luyendyk, B.P., 2004, Ross Sea mylonites and the timing of intracontinental extension within the West Antarctic rift system: Geology, v. 32, no. 1, p. 57–60, https://doi.org/10.1130/G20005.1.

Sieminski, A., Debzyle, E., and Leveque, J.-J., 2003, Seismic evidence for deep low-velocity anomalies in the transition zone beneath West Antarctica: Earth and Planetary Science Letters, v. 216, p. 645–661, https://doi.org/10.1016/S0012-821X(03)00518-1.

Sleep, N.H., 1992, Hotspot volcanism and mantle plumes: Annual Review of Earth and Planetary Sciences, v. 20, p. 19–43, https://doi.org/10.1146/annurev.ea.20.050192.000315.

Storey, B.C., Alabaster, T., Hole, M.J., Pankhurst, R.J., and Weaver, H.E., 1992, Role of subduction-plate boundary forces during the initial stages of Gondwana break-up: Evidence from the proto-Pacific margin of Antarctica, in Storey, B.C., Alabaster, T., and Pankhurst, R.J., eds., Magmatism and the Causes of Continental Breakup: Geological Society of London Special Publication 68, p. 149–163, https://doi.org/10.1144/GSL.SP1992.068.01.10.

Storey, B.C., Leat, P.T., Weaver, S.D., Pankhurst, R.J., Bradshaw, J.D., and Kelley, S., 1999, Mantle plumes and Antarctica-New Zealand rifting: Evidence from mid-Cretaceous mafic dykes: Journal of the Geological Society, v. 156, p. 659–671, https://doi.org/10.1144/gsjgs.156.4.0659.

Storti, F., Balestrieri, M.L., Balsamo, F., and Rossetti, F., 2008, Structural and thermochronological constraints to the evolution of the West Antarctic Rift System in central Victoria Land: Tectonics, v. 27, no. 2, TC4012, https://doi.org/10.1029/2006TC002066.

Studinger, M., Bell, R.E., Buck, W.R., Karner, G.D., and Blankenship, D.D., 2004, Sub-ice geology inland of the Transantarctic Mountains in light of new aerogeophysical data: Earth and Planetary Science Letters, v. 220, p. 391–408, https://doi.org/10.1016/S0012-821X(04)00066-4.

Studinger, M., Bell, R.E., Fitzgerald, P.G., and Buck, R.W., 2006, Crustal architecture of the Transantarctic Mountains between the Scott and Reedy Glacier region and South Pole from aerogeophysical data: Earth and Planetary Science Letters, v. 250, p. 182–199, https://doi.org/10.1016/j.epsl.2006.07.035.

Tonarini, S., Rocchi, S., Aremienti, P., and Innocenti, F., 1997, Constraints on timing of Ross Sea rifting inferred from Cenozoic intrusions from northern Victoria Land, Antarctica, in Ricci, C.A., ed., The Antarctic Region: Geological Evolution and Processes: Siena, Italy, Terra Antarctica Publications, p. 511–521.

Torsvik, T.H., Gaina, C., and Refield, T.F., 2008, Antarctica and global paleogeography: From Rodinia, through Gondwanaland and Pangea, to the birth of the Southern Ocean and the opening of gateways, in Cooper, A.K., Barrett, P.J., Stagg, H., Storey, B., Stump, E., Wise, W., Anderson, J., Barron, J., Bart, P., Blankenship, D., Davey, F., Diggles, M., Finn, C., Fitzgerald, P., Florindo, F., Francis, J., Futterer, D., Gamble, J., Goodge, J., Hammer, W., Helton, P., Ivins, E., Kyle, P., LeMasurier, W., Mayewski, P., Naish, T., Passchier, S., Pekar, S., Raymond, C., Ricci, C.A., Studinger, M., Sugden, D., Thorn, V., and Wilson, T., eds., Antarctica: A Keystone in a Changing World: Washington, D.C., USA, The National Academies Press Proceedings of the 10th International Symposium on Antarctic Earth Sciences, p. 125–140.

Trey, H., Cooper, A.K., Pellis, G., Vedova, B.d., Cochrane, G., Brancolini, G., and Makris, J., 1999, Transect across the West Antarctic rift system in the Ross Sea, Antarctica: Tectonophysics, v. 301, p. 61–74, https://doi.org/10.1016/S0040-1951(98)00155-3.

van Wijk, J.W., and Cloetingh, S.A.P.L., 2002, Basin migration caused by slow lithospheric extension: Earth and Planetary Science Letters, v. 198, p. 275–288, https://doi.org/10.1016/S0012-821X(02)00560-5.

van Wijk, J.W., Lawrence, F., and Driscoll, N.W., 2008, Formation of the Transantarctic Mountains related to extension of the West Antarctic Rift system: Tectonophysics, v. 458, p. 117–126, https://doi.org/10.1016/j.tecto.2008.03.009.

Vedova, B.D., Pellis, G., Lawver, L.A., and Brancolini, G., 1992, Heat flow and tectonics of the western Ross Sea, in Yoshida, Y., Kaminuma, K., and Shiraishi, K., eds., Recent Progress in Antarctic Earth Science: Tokyo, Japan, Terra Scientific Publishing Company, p. 627–637.

von Frese, R.R.B., Tan, L., Kim, J.W., and Bentley, C.R., 1999, Antarctic crustal modeling from the spectral correlation of free-air gravity anomalies with the terrain: Journal of Geophysical Research, v. 104, no. 11, p. 25275–25296, https://doi.org/10.1029/1999JB900232.

Watson, T., Nyblade, A., Wiens, D.A., Anandakrishnan, S., Benoit, M., Shore, P.J., Voigt, D., and VanDecar, J., 2006, P and S velocity structure of the upper mantle beneath the Transantarctic Mountains, East Antarctic craton, and Ross Sea from travel time tomography: Geochemistry, Geophysics, Geosystems, v. 7, no. 7, p. https://doi.org/10.1029/2005GC001238.

Weaver, S.D., Storey, B.C., Pankhurst, R.J., Mukasa, S.B., DiVenere, V.J., and Bradshaw, J.D., 1994, Antarctica–New Zealand rifting and Marie Byrd Land lithospheric magmatism linked to ridge subduction and mantle plume activity: Geology, v. 22, p. 811–814, https://doi.org/10.1130/0091-7613(1994)022<0811:ANZRAM>2.3.CO;2.

White, R., and McKenzie, D., 1989, Magmatism at rift zones: The generation of volcanic continental margins and flood basalts: Journal of Geophysical Research, v. 94, p. 7685–7729, https://doi.org/10.1029/JB094iB06p07685.

Wilson, D.S., and Luyendyk, B.P., 2009, West Antarctic paleotopography estimated at the Eocene-Oligocene climate transition: Geophysical Research Letters, v. 36, L16302, https://doi.org/10.1029/2009GL039297.

Wilson, D.S., Jamieson, S.S.R., Barrett, P.J., Leitchenkov, G., Gohl, K., and Larter, R.D., 2012a, Antarctic topography at the Eocene-Oligocene Boundary: Palaeogeography, Palaeoclimatology, Palaeoecology, v. 335–336, p. 24–34, https://doi.org/10.1016/j.palaeo.2011.05.028.

Wilson, G.S., Roberts, A.P., Verosub, K.L., Florindo, F., and Sagnotti, L., 1998, Magnetobiostratigraphic chronology of the Eocene–Oligocene transition in the CIROS-1 core, Victoria Land margin, Antarctica: Implications for Antarctic glacial history: Geological Society of America Bulletin, v. 110, p. 35–47, https://doi.org/10.1130/0016-7606(1998)110<0035:MCOTEO>2.3.CO;2.

Wilson, G.S., Levy, R.H., Naish, T.R., Powell, R.D., Florindo, F., Ohneiser, C., Sagnotti, L., Winter, D.M., Cody, R., Henrys, S., Ross, J., Krissek, L., Niessen, F., Pompillio, M., Scherer, R., Alloway, B.V., Barrett, P.J., Brachfeld, S., Browne, G., Carter, L., Cowan, E., Crampton, J., DeConto, R.M., Dunbar, G., Dunbar, N., Dunbar, R., von Eynatten, H., Gebhardt, C., Giorgetti, G., Graham, I., Hannah, M., Hansaraj, D., Harwood, D.M., Hinnov, L., Jarrard, R.D., Joseph, L., Kominz, M., Kuhn, G., Kyle, P., Läufer, A., McIntosh, W.C., McKay, R., Maffioli, P., Magens, D., Millan, C., Monien, D., Morin, R., Paulsen, T., Persico, P., Pollard, D., Raine, J.I., Riesselman, C., Sandroni, S., Schmitt, D., Sjunneskog, C., Strong, C.P., Talarico, F., Taviani, M., Villa, G., Vogel, S., Wilch, T., Williams, T., Wilson, T.J., and Wise, S., 2012b, Neogene tectonic and climatic evolution of the Western Ross Sea, Antarctica—Chronology of events from the AND-1B drill hole: Global and Planetary Change, v. 96–97, p. 189–203, https://doi.org/10.1016/j.gloplacha.2012.05.019.

Wilson, T.J., 1995, Cenozoic transtension along the Transantarctic Mountains-West Antarctic rift boundary, southern Victoria Land, Antarctica: Tectonics, v. 14, p. 531–545, https://doi.org/10.1029/94TC02441.

Winberry, J.P., and Anandakrishnan, S., 2004, Crustal structure of the West Antarctic rift system and Marie Byrd Land hotspot: Geology, v. 32, no. 11, p. 977–980, https://doi.org/10.1130/G20768.1.

Wörner, G., 1999, Lithospheric dynamics and mantle sources of alkaline magmatism of the Cenozoic West Antarctic Rift System: Global and Planetary Change, v. 23, p. 61–77, https://doi.org/10.1016/S0921-8181(99)00051-X.